CrossMark

RESEARCH PAPER

Shear wave velocity as function of cone penetration resistance and grain size for Holocene-age uncemented soils: a new perspective

Mourad Karray[1] · Mahmoud N. Hussien[1,2]

Abstract For feasibility studies and preliminary design estimates, field measurements of shear wave velocity, V_s, may not be economically adequate and empirical correlations between V_s and more available penetration measurements such as cone penetration test, CPT, data turn out to be potentially valuable at least for initial evaluation of the small-strain stiffness of soils. These types of correlations between geophysical (Vs) and geotechnical (N-SPT, q_c-CPT) measurements are also of utmost importance where a great precision in the calculation of the deposit response is required such as in liquefaction evaluation or earthquake ground response analyses. In this study, the stress-normalized shear wave velocity V_{s1} (in m/s) is defined as statistical functions of the normalized dimensionless resistance, Q_{tn}-CPT, and the mean effective diameter, D_{50} (in mm), using a data set of different uncemented soils of Holocene age accumulated at various sites in North America, Europe, and Asia. The V_{s1}–Q_{tn} data exhibit different trends with respect to grain sizes. For soils with mean grain size (D_{50}) < 0.2 mm, the $V_{s1}/Q_{tn}^{0.25}$ ratio undergoes a significant reduction with the increase in D_{50} of the soil. This trend is completely reversed with further increase in D_{50} (D_{50} > 0.2 mm). These results corroborate earlier results that stressed the use of different CPT-based correlations with different soil types, and those emphasized the need to impose particle-size limits on the validity of the majority of available correlations.

✉ Mourad Karray
  Mourad.Karray@Usherbrooke.ca

  Mahmoud N. Hussien
  Mahmoud.Nasser.Ahmed@USherbrooke.ca

1 Department of Civil Engineering, Université de Sherbrooke, Sherbrooke, QC J1K 2R1, Canada

2 Department of Civil Engineering, Faculty of Engineering, Assiut University, Assiut, Egypt

1 Introduction

Shear wave velocity, V_s is a key parameter required to effectively define the dynamic characteristics of soils. The importance of V_s has been widely recognized in ground motion prediction equations by implementation of site factors that modify ground motion based on the difference between a site V_s and a reference V_s (typically for rock, e.g., [18]), or by direct incorporation of a V_s term in the ground motion regression equations [14]. Shear wave velocity has been also used to evaluate liquefaction potential (e.g., [2, 3]). In addition to dynamic applications, V_s has been used for the assessment of deep compaction and in situ evaluation of hard-to-sample deposits and, eventually, for the identification of bedrock position (e.g., [51]). For these reasons, the demand for a precise site investigation for V_s profiling is increasing rapidly in the field of geotechnical engineering.

In situ measurements of V_s using geophysical methods are now customary for geotechnical projects where vibrations are expected. These methods include borehole methods (cross-hole, down-hole, and up-hole), the seismic cone penetration test (SCPT), and the analysis of surface waves (i.e., spectral analysis of surface waves (SASW) and multi-modal analysis of surface waves (MMASW)). In fact, the direct measurement of V_s using one of these methods requires specialized equipment and technical proficiency to ensure that the data are correctly obtained and interpreted. In order to optimize the existing V_s measurements, several researchers and practitioners have

🖄 Springer

examined the viability of correlations between V_s and CPT data (e.g., [6, 52, 76]). Although direct measurements of V_s are always favored over estimates, correlations with penetration resistance are potentially valuable in the following cases [4, 29, 39, 53, 101]:

- To provide an order-of-magnitude check versus measured shear wave velocities;
- For feasibility studies and preliminary designs, before any field or laboratory measurements have been executed;
- For final design calculations in low-risk projects where the costs of an appropriate testing for V_s are not justified; and
- For developing regional ground-shaking hazard maps when the number of existing V_s measurements is limited. Correlations with the more ample penetration data can offer timely and economical contributions required for regional and preliminary site-specific ground responses analyses.
- To verify the coherence between the obtained geophysical (V_s) and geotechnical (N-SPT, q_c-CPT) measurements where a great precision in the calculation of the deposit response is required such as in liquefaction evaluation or earthquake ground response analyses.

A matter of concern with estimating V_s from cone penetration resistance q_c-CPT is that the former is a small-strain parameter, whereas the latter is an ultimate strength measurement. Therefore, the factors dominating the soil behavior at small and large strains may be quite different. The issue was abundantly discussed by Mayne and Rix [68] and has been later supported by Schneider et al. [90]. In particular, [90], based on microscale interpretation of mechanisms controlling wave propagation [88] and cone penetration in sands, concluded that V_s of sands is dominated by the number and area of grain-to-grain contacts that in turn depends on void ratio, effective stress state, cementation, and rearrangement of particles with time. On the other hand, penetration resistance in sands is governed by the interaction of particles being sheared by and rotating around the penetrometer. The latter behavior depends primarily on relative density and effective stress state, particularly in the horizontal direction, and to a lesser degree by cementation and age [4]. In other words, q_c and V_s, though reflecting soil behavioral responses at opposite ends of the strain spectrum, reveal a functional dependence on similar quantities (i.e., confining stress level, relative density or void ratio, geologic age, mineralogy) and thus can be legitimately assumed to correlate [99].

Over the past years, a substantial research effort has been conducted to develop correlations between V_s and cone tip resistance (q_c). These efforts have demonstrated that cone sleeve friction, confining stress, depth, soil type,

and geologic age are factors influencing the correlation. Likewise, the accumulated experience gained so far on such correlations has obviously shown that fine and coarse granular soils generally follow different trends. Robertson [78, 79], Karray et al. [52], and Karray and Éthier [49] have stressed the role of particle-size distribution, suggesting the use of relations where the ratio between the stress-normalized shear wave velocity V_{s1} and the stress-normalized dimensionless penetration resistance Q_{tn}, for granular material, is assumed to vary with the mean grain size, D_{50} or the Soil Behavior Type (SBTn) Index, I_c (I_c is inversely proportional to grain size). However, their results are inconsistent with respect to the effects of grain size on the V_{s1}/Q_{tn} ratio. Using the Péribonka project data obtained on fairly coarse sands in conjunction with CANLEX project data obtained on fine sands, Karray et al. [52] suggested an increase in V_{s1}/Q_{tn} ratio with the increase in D_{50}. However, Robertson [79], based on Andrus et al. [4] data from a wide range of soil type, including cohesive and non-cohesive materials, reported a reduction in V_{s1}/Q_{tn} ratio with the decrease in I_c (i.e., as the soil becomes more coarse grained). Figure 1 compares the Karray et al. [52] relationship with the range of data from Andrus et al. [4] (assuming the stress-normalized cone tip resistance q_{c1N} is equal to the more general form for the normalized cone tip resistance, Q_{tn} as suggested by Robertson [79] for sandy soils). The Karray et al. [52] relationship indicates that for a given normalized shear wave velocity, the normalized cone resistance decreases as D_{50} increases. This would appear to be different to the trend of data from Andrus et al. [4] and the relationship suggested by Robertson [79] which was based on a wider range of soil types and grain sizes. Indeed, the Péribonka project is a very important site including a bank of data (1084 data pairs) of coarse gravelly sand from a direct profile-to-profile comparison at 100 or so locations on the site. As far as the authors know, this site comprises a unique database, and it is hard to dogmatize that the relationship based on Péribonka data is odd to the well-known correlations of Andrus et al. [4] and Robertson [79]. What can be asserted right now based of course on the available information from both the opposing sides presented in Fig. 1 is that the Karray et al. [52] formulation is preponderating by coarse-grained soils and should be applied on soils with D_{50} higher than 0.2 mm as discussed by Prof. Robertson [79]. On the other hand, data of Andrus et al. [4] and Robertson [79] are more weighted toward fine-grained soils. Compared to the Péribonka project data, Andrus et al.'s [4] data do not, in fact, contain substantial information on the V_{s1}/Q_{tn} ratio of coarse gravelly sand. To disentangle the issue even partially, V_{s1}–Q_{tn} data obtained from other well-documented experimental tests by Suzuki et al. [96] with comparable grain sizes are plotted in Fig. 1. It is interesting to note from
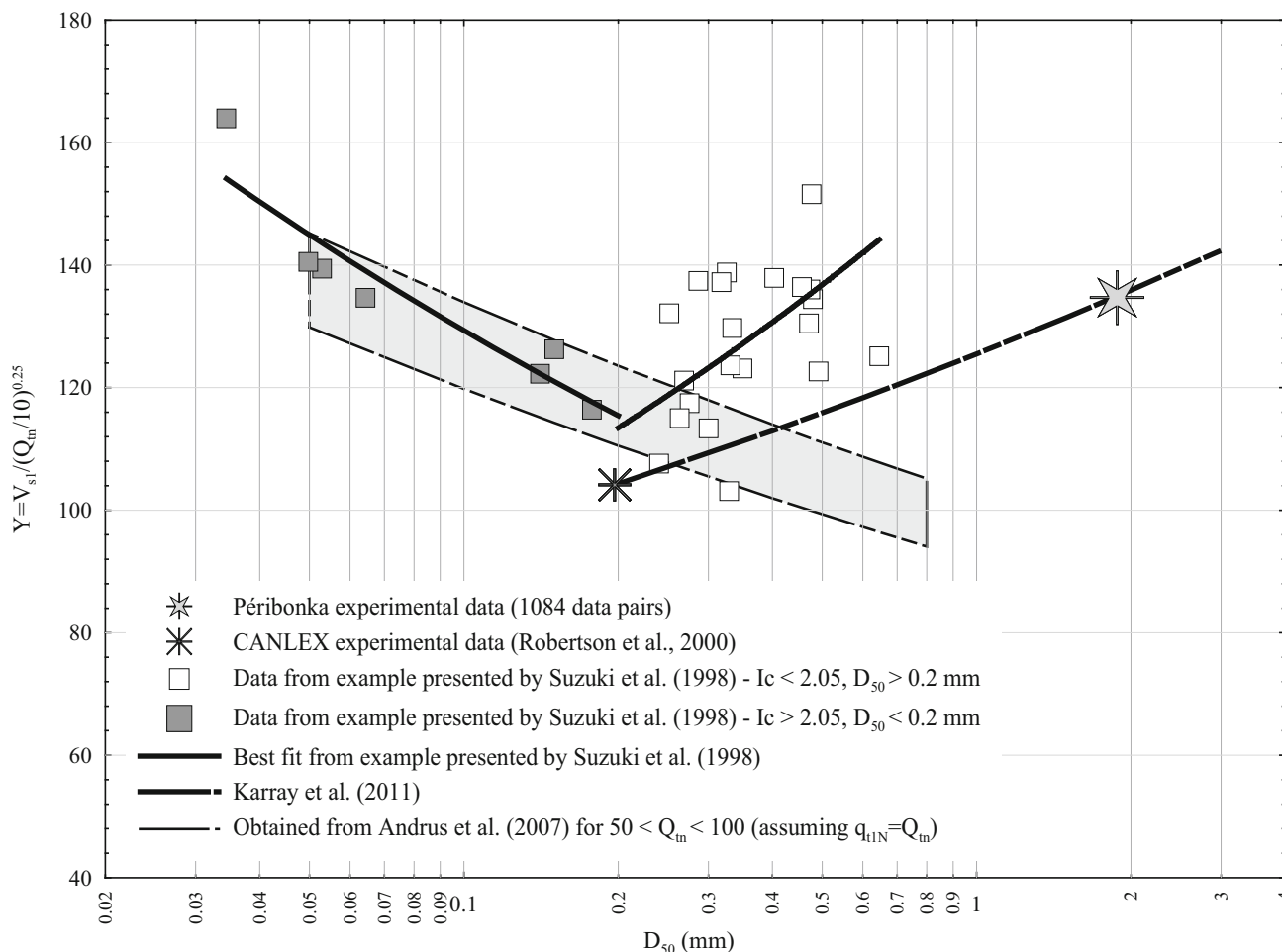
Fig. 1 Comparative $V_{s1}/(Q_{tn}/10)^{0.25}$–$D_{50}$ results reported by Karray et al. [52] based on Péribonka data and [4] as well as [96]

Fig. 1 that part of the newly introduced experimental data ($D_{50} < 0.2$ mm) fall in the same range suggested by Andrus et al. [4] and Robertson [79], while the other part of data ($D_{50} > 0.2$ mm) follows, to some extent, the Karray et al. [52] trend. In fact, this aspect of soil behavior with respect to the effect of grain size (D_{50}) on V_{s1}/Q_{tn} trend has not explicitly studied in research and consequently not fully understood.

In this study, based on a wide range of well-documented case histories on different uncemented soils of Holocene age (< 10,000 years) at various sites in the USA, Canada, Norway, Italy, Ireland, Taiwan, and Hong Kong, the stress-normalized shear wave velocity V_{s1} (in m/s) is defined as statistical functions of the normalized dimensionless cone penetration resistance, Q_{tn}-CPT, and the mean effective diameter, D_{50} (in mm). These sites are carefully selected among other sites such that at each selected site, the V_{s1}–Q_{tn} correlation is derived from data of the same soundings with particle-size determination, and additional uncertainties induced by spatial variability are thus eliminated. Particular emphasis is placed in this article on the

validation of the proposed correlations through: (1) comparing the calculated V_{s1} based on the proposed correlations with reliable laboratory V_{s1} measurements; (2) examining the compatibility between correlations of liquefaction potential based on the proposed formulations and various liquefaction charts established in the literature. Moreover, V_s profiles computed using the proposed formulations are compared favorably with field data at three different sites. The use of the new field data, which were obtained also under controlled conditions, provides independent trials of the proposed formulations.

2 Basic state of knowledge

In situ testing of soil beds by the penetration of cones is the most effective and universal method of acquiring a large volume of data on the stratification and mechanical properties of soils. The CPT involves pushing an instrumented cone penetrometer into the ground and measuring the cone tip resistance (q_c) and sleeve friction (f_s) at selected depths.

The three most common CPT systems used for geotechnical site investigation are the conventional CPT, the piezo-CPT (CPTu), and seismic CPT (SCPT). In particular, the CPTu is now required by ASTM D5778-12 [5] as the pore pressure readings allow the measured q_c to be corrected to the total cone resistance, q_t. A major advantage of the seismic CPT (SCPT) over traditional methods of field site investigation is that the additional measurement of V_s is measured using a down-hole technique during pauses in the CPT resulting in a continuous profile of V_s. Due to the growing use of CPTu/SCPT, huge amounts of data on various soil types have been collected worldwide; hence, the possibility of deriving reliable values of the seismic properties of soils from conventional cone penetration readings provides an interesting and economical way of optimizing the existing measurements [99]. In this context, V_s can be efficiently correlated with q_c-CPT in conjunction with soil type that can be expressed, for example, in terms of the Soil Behavior Type (SBTn) Index (I_c) first introduced by Jefferies and Davies [48], as well as a discussion of theirs [47] to the [77] paper. The use of I_c into cone penetration-based empirical correlations has been investigated by various authors, and its effectiveness in reflecting the different mechanical behaviors of soils, together with the ability of allowing a unified description of soil response, is now widely acknowledged (e.g., [57, 78]).

A significant number of empirical correlations between V_s and CPT results have been proposed in the literature following the pioneering studies of Baldi et al. [7], Bouckovalas et al. [11] Jamiolkowski et al. [45], and Mayne and Rix [68]. Table 1 summarizes the pertinent details of some of these correlations, including locations/countries, number of data pairs, geologic age, and method of V_s measurement. These correlations explore the relationships between V_s and various parameters, including q_c, f_s, I_C, effective vertical stress (σ'_v), depth, and soil type. For consistency, the equations have been adjusted to use consistent units. V_s is presented in m/s, $q_c, f_s,$ and σ'_v are presented in kPa, depth is presented in meters, and D_{50} is presented in mm. Correlation equations presented in Table 1 were generally developed for specific soils types (i.e., "Sand" or "Clay") or grouped together as "All soils." Most V_s–q_c correlations are characterized by their lack of dependence on effective stress or depth. However, limited correlations use stress-corrected quantities for both V_s and q_c, so as to remove the effect of overburden pressure. V_s is routinely normalized for a vertical effective stress, σ'_v, as in studies for the evaluation of the liquefaction potential (e.g., [103]).

$$V_{s1} = V_s \left(\frac{P_a}{\sigma'_v}\right)^{0.25} \quad \text{(m/s)} \tag{1}$$

where V_{s1} is the vertical stress-normalized shear wave velocity, and P_a is a reference pressure in the same units as σ'_v (i.e., Pa = 100 kPa if σ'_v is in kPa).

In some correlations in Table 1, the cone tip resistances were corrected for the effect of pore water pressure acting behind the tip. The corrected tip resistance (q_t) can be calculated by:

$$q_t = q_c + (1 - a_n) \cdot u_2 \tag{2}$$

where u_2 is the measured pore pressure, and a_n is the ratio between shoulder area (cone base) unaffected by the pore water pressure to total shoulder area. Typical values of a_n range from 0.5 to 1.0 [63]. Similar to the overburden stress correction used for V_s, the effect of overburden stress on q_t can be removed [77]:

$$Q_t = \left(\frac{(q_t - \sigma_v)}{\sigma'_v}\right) \tag{3}$$

where Q_t is the dimensionless stress-normalized cone penetration resistance and σ_v is the total vertical stress. Robertson and Wride [82] and the update by Zhang et al. [104] suggested a more general form for the normalized cone resistance with a variable stress exponent, n, where:

$$Q_{tn} = \left(\frac{(q_t - \sigma_v)}{P_a}\right) \cdot \left(\frac{P_a}{\sigma'_v}\right)^n \tag{4}$$

where $(q_t - \sigma_v)/P_a$ is the dimensionless net cone resistance, $(P_a/\sigma'_v)^n$ is the stress normalization factor, and n is the stress exponent that varies with SBTn. Robertson [78] suggested also a simplified iterative approach to evaluate the exponent n in Eq. 4 which is typically equal to 1.0 for soil classification in clay-type soils and 0.5 for granular type soils.

The sleeve friction measured during penetration in the CPT test, f_s, can be normalized with respect to the corrected net tip resistance ($q_t - \sigma_v$) as [77]:

$$F = \frac{f_s}{q_t - \sigma_v} \cdot 100\% \tag{5}$$

where F is the standardized friction ratio.

The use of the net cone resistance ($q_t - \sigma_v$) in Eqs. 3 and 4 is important in clay soils, but less so in dense sandy soils [79], and the normalized cone tip resistance for sandy soil can be defined by Robertson and Wride [82]:

$$q_{c1N} = \left(\frac{q_c}{P_a}\right) \cdot \left(\frac{P_a}{\sigma'_v}\right)^{0.5} \tag{6}$$

and

$$q_{c1} = q_c \cdot \left(\frac{P_a}{\sigma'_v}\right)^{0.5} \tag{7}$$

Table 1 Existing correlations between V_s and CPT data

Author(s)	Type of soil	Geologic age	No. of data pairs	Correlation	Correlation coefficient	Method of V_s measurement	Country
Hegazy and Mayne [38]	All soils	Quaternary	323	$V_s = (10.1 \log(q_c) - 11.4)^{1.67}(100\, f_s/q_c)^{0.3}$	0.70	Cross-hole, down-hole, SCPT, SASW	Worldwide
	Sands		92	$V_s = 12.02 q_c^{0.319} f_s^{-0.0466}$	0.57		
	Clays		229	$V_s = 3.18 q_c^{0.549} f_s^{0.025}$	0.78		
Mayne [66]	All soils	Quaternary	161	$V_s = 118.8 \log(f_s) + 18.5$	0.82	Cross-hole, down-hole, SCPT, SASW	Worldwide
Piratheepan [75]	All soils	Holocene	60	$V_s = 32.3 q_c^{0.089} f_s^{0.121} D^{0.215}$	0.73	n/a	USA, Japan, Canada
	Sands		25	$V_s = 25.3 q_c^{0.163} f_s^{0.029} D^{0.155}$	0.74		
	Clays		20	$V_s = 11.9 q_c^{0.269} f_s^{0.108} D^{0.127}$	0.91		
Robertson et al. [84]	Sands	Holocene	n/a	$V_{s1} = 20.83 q_{c1}^{0.25}$	n/a	SCPT	Canada
Fear and Robertson[27]	Sands	n/a	n/a	$V_{s1} = 27.56 q_{c1}^{0.25}$	n/a	n/a	USA
Sykora and Stokoe [98]	Sands	n/a	256	$V_s = 134.1 + 0.0052 q_c$	0.61	Cross-hole	USA
Baldi et al. [7]	Sands	Holocene	n/a	$V_s = 17.48 q_c^{0.13} \sigma_v'^{0.27}$	n/a	Resonant column	Italy
Mayne and Rix [69]	Clays	Quaternary	481	$V_s = 1.75 q_c^{0.627}$	0.74	Cross-hole, down-hole, SCPT, SASW	Worldwide
Wride et al. [102]	Fine sand $0.16 < D_{50} < 0.25$	Holocene	n/a	$V_{s1} = Y q_{c1}^{0.25}$ $(17 \leq Y \leq 19.7)$	n/a	SCPT	CANLEX project
Andrus et al. [4]	Sands	Holocene	72	$V_{s1} = 16.5 q_{t1N}^{0.411} I_c^{0.970}$	0.71	SCPT, Cross-hole	USA, Japan
Robertson [78]	All soils	Holocene and Pleistocene	1035	$V_{s1} = \left[(10^{(0.55 I_c + 1.68)})(q_t - \sigma_v)/p_a\right]^{0.5}$	n/a	SCPT	Worldwide
Karray et al. [52]	Granular soils $0.2 < D_{50} < 10$	Holocene	1084	$V_{s1} = 125.5 q_{c1N}^{0.25} D_{50}^{0.115}$	n/a	MMASW	Péribonka dam, Canada
Robertson [79]	All soils	Holocene and Pleistocene	1035	$V_{s1} = \left[(10^{(0.55 I_c + 1.68)}) q_{c1N}\right]^{0.5}$	n/a	SCPT	Worldwide
Tonni and Simonini[99]	Sands and silts	Holocene	n/a	$V_{s1} = (10^{(0.37 I_c + 0.63)}) Q_{tn}^{0.5}$	0.79	SCPT	Italy

V_s and V_{s1} are presented in m/s; q_c, q_t, q_{c1}, f_s, and σ_v' are presented in kPa; depth, D is presented in meters; and effective mean diameter, D_{50}, is presented in mm. $p_a = 100$ kPa; q_{c1N}, q_{t1N}, Q_{tn}, and I_c are dimensionless quantities

where $q_{c1} = q_{c1N} P_a$.

V_s–q_c correlations presented in Table 1 did not follow a single pattern and contain different numbers of correlative variables. In other words, some of the correlations contain two correlative variables (e.g., [66, 69]), while other contain four variables (e.g., [38, 78]). Field experience indicates also that V_s–q_c correlations vary in their reliability and applicability. Such variability suggests that some site-specific V_s measurements may be required to make accurate predictions of V_s from CPT results. In fact, some empirical relationships contain no function taking into account the particle characteristics (e.g., particle size, particle shape, particle gradation, and mineral composition), and/or they did not impose particle-size limits for the validity of the proposed relationship. Other correlations, however, emphasize on the effect of particle-size distribution, for instance the effect of the fine fraction, mean grain size (D_{50}), or gravel fraction. Robertson [77], however, proposed a unified correlation and suggested a normalized soil classification system chart based on the normalized tip resistance (Q_t) and normalized friction ratio (F). A modified version of the I_c of Jefferies and Davies [48] is suggested by Robertson et al. [64, 82] to be applied to the [77] Q_t-F chart, as defined by:

$$I_c = \left[(3.47 - \log Q_{tn})^2 + (\log F + 1.22)^2 \right]^{0.5} \quad (8)$$

It is worthy of note that the definition of I_c suggested by Robertson and co-workers (Eq. 8) will be used throughout the current paper. The Robertson chart, later updated by Robertson [78], makes it possible to classify the soil in nine categories ranging from sensitive, fine-grained soil to gravelly soil. The categories for normally consolidated soil generally increase with the decrease in the soil behavior index, I_c. However, the accuracy of these types of global correlations (determined based on statistical regression of a wide range of data set, soil types, and conditions) may be questionable as it is established that divisions of data among different soil types improved the accuracy of correlative equations as will be discussed next.

2.1 Grain size and geotechnical parameters (V_s, N-SPT and q_c-CPT): a review

It is well recognized that void ratio (e), effective stress, (σ_v'), and relative density (I_D) greatly affect both strength (e.g., standard penetration test blow count, N-SPT, and cone penetration resistance, q_c-CPT) and stiffness (e.g., V_s) parameters of soils. However, few recommendations are given in the literature on how to consider the influence of the mean grain size (D_{50}) of soils when estimating these parameters or constructing correlations between them. Hardin [34] noted that V_s of two different soils (i.e., dense

crushed quartz and loose Ottawa sand) having similar D_{50} was the same. He further concluded that V_s at $I_D = 100\%$ might be different for two sands; however, at the same void ratio, V_s should be relatively similar. Hardin and Richart [36] confirmed that the values V_s of different soils with different D_{50} at the same I_D and effective stress may be quite different. They reported also that different soils will have essentially the same V_s at the same void ratio as the major effect of grain size and gradation was to change the range of possible void ratios which in turn had a significant impact on V_s. In other words, soils with finer relative grain size distributions have a larger e, and, therefore, lower V_s. Iwasaki and Tatsuoka [42], based on resonant column (RC) tests on normally consolidated reconstituted sands with different D_{50}, reported that V_s of sand is strongly affected by the grain size distribution characteristics. Sykora [97] analyzed data from previous studies and pointed out that the upper and lower bounds of V_s per study increase with the increase in relative grain size (i.e., clay, sand, gravel, respectively). He pointed out also that soils with wide ranges of grain sizes tend to have smaller average void ratios and, therefore, exhibit larger values of V_s. Ishihara [41] collected V_s values for various sands and gravels tested in Japan in the 1980s with different values of particle sizes and void ratios and suggested that there is a significant difference in V_s values for different types of gravel (e.g., $V_{s(crushed\ rocked)} > V_{s(gravel)} > V_{s(sandy\ gravel)}$). Rollins et al. [87], through tests in which the content of gravel was increased from 0 to 60%, confirmed that V_s increases with gravel content. Hardin and Kalinski [35], using a special large-scale torsional RC apparatus, performed 17 tests on different sands and sand–gravel mixtures. G_{max} of the gravels was found to be significantly larger than those of the uniform sands.

Dodds [23] performed bender element (BE) tests to measure V_s of crushed granite materials with uniform grain size distribution ($2.5 < C_u < 4.0$) and different values of D_{50}. He presented his results using the velocity–stress power relationship for granular media [86, 89] as:

$$V_s(\text{m/s}) = \alpha \left[\frac{\sigma_0'}{1\ \text{kPa}} \right]^{\beta = (0.36 - \alpha/700)} \quad (9)$$

where α and β are experimentally determined parameters and σ_0' is the effective confining pressure. The results of Dodds [23] show quantitatively that the parameter α and consequently V_s increase with increasing D_{50} as:

$$\alpha = 200D_{50} - 18.5 \text{ for } 0.25 < D_{50} < 0.42 \quad (10)$$

Menq [71] conducted RC tests to measure the values of the small-strain shear modulus, G_{max} ($G_{max} = \rho V_s^2$, ρ is the density), of 59 reconstituted specimens of natural river sands with D_{50} varying from 0.11 to 17.4 mm, C_u

(coefficient of uniformity) varying between 1.1 and 15.9, and dry density expressed in terms of void ratio with values varying from 0.38 to 1.15. For constant mean effective stress and void ratio, [71] reported an increase in G_{max} with increasing D_{50} and C_u and proposed the following correlation:

$$G_{max}(MPa) = 67.1 e^{-(1.3+(D_{50}/12))^{0.82}} \left(\frac{\sigma'_0}{P_a}\right)^{0.48 C_u^{0.09}} / C_u^{0.2} \quad (11)$$

It can be shown, using this relationship, that an increase in D_{50} from 0.2 (fine-grained granular soil) to 3.0 mm (coarse-grained granular soil) at constant C_u, e, and σ'_0 produces an increase in G_{max} of about 9%. In other words, this equation shows that at the same void ratio, V_s of the soil increases slightly with the increase in its mean grain size. However, when compared in terms of I_D, Menq's results show clearly that the effect of grain size is much more pronounced. His results showed that the ratio between G_{max} of course granular soils ($D_{50} \approx 3.0$ mm) and that of finer soils ($D_{50} \approx 0.2$ mm) reconstituted at the same I_D is about 1.6 in accord with the results of Hanna et al. [33], indicating that V_s is a function of I_d. Bui [16] observed an increasing of G_{max} value by about 25% between coarse ($D_{50} = 3$ mm) and fine-grained soils ($D_{50} = 0.1$ mm) at the same void ratio. Bui [16] attributed the grain size effect to the decrease in the contact per unit solid volume as well as to the increase in contact area and consequently contact force leading to the increase in friction strength and hence contact stiffness. Fumal and Tinsley [28] presented the values of shear wave velocities measured at the Los Angeles basin subarea. As shown in Table 2, these data are divided according to grain size distribution into four categories: (1) fine, (2) medium, (3) coarse, and (4) very coarse. The data illustrate that V_s increases as the grain size increases, and the ratio of G_{max} of coarse- and fine-grained soils is about 2.5.

The results available in the literature with regard to the effect of grain size on N-SPT or q_c-CPT are fairly more. For example, [21] reported that at a given I_d and overburden pressure, N-values are higher for sands with larger grain sizes (D_{50}) consistent with the results of other researchers such as [94] and [58] who suggested the following relationships:

$$(N_1)_{60}/I_D^2 = 60 + 25 log D_{50} \quad (12)$$

where $N_{1(60)}$ is the blow count corrected for the effective stress and energy level used in the SPT and I_D is expressed as a decimal. Ohta and Goto [74] showed that the ratio V_s/N varies with soil type according to:

$$\left(\frac{V_s}{N^{0.22} . H^{0.23}}\right) = X \quad (13)$$

where V_s is in m/s, and H is the depth below ground surface in m. The values of X for cohesionless soil are 67.79 for fine sand, 63.94 for medium sand, 66.68 for coarse sand, 71.52 for gravelly sand, and 92.28 for gravel. These results indicate clearly that the V_s/N ratio increases with increasing grain size in general and also imply that V_s is more sensitive than N with respect to grain size. In the same context, a number of studies have been presented over the years to correlate the (q_c/N) ratio with D_{50} for a variety of soil types. Robertson and Campanella [81] reviewed these correlations and observed that the ratio increases with increasing grain size. Robertson et al. [83] suggested values of (q_c/p_a)/N ratios for each soil type. Suzuki et al. [96] showed that the ratio q_c/N varies with fines content and relative density. Other correlations have been proposed (e.g., [1, 58, 70, 73]). For example, [70] reported the following equation:

$$\left(\frac{q_{c1N}}{(N_1)_{60}}\right) \approx 5.44(D_{50})^{0.26} \quad (14)$$

The variation of $q_{c1N}/N_{1(60)}$ ratio with main grain size, D_{50}, can be also expressed according to [1] as:

$$\frac{q_{c1N}}{N_{1(60)}} \approx 7.6429 D_{50}^{0.26} \quad (15)$$

where $(N_1)_{60}$ is the standard penetration test blow count corrected for hammer energy, rod length, and sampler inside diameter; D_{50} is given in mm. In fact, both $(N_1)_{60}$ and q_{c1N} increase with the increase in grain size, and q_{c1N} is more sensitive to the change in particle size.

Moreover, [58] suggested an equation to estimate the relative density of the soil from its cone resistance as:

$$I_D^2 = \frac{1}{305 Q_c OCR^{0.18}} \frac{q_c/P_a}{(\sigma'_v/P_a)^{0.5}} \quad (16)$$

where Q_c is the compressibility factor ranging from 0.90 to 1.10, OCR is the overconsolidation ratio, and I_D is expressed as a decimal. Equation 16 can be simplified for most young, uncemented silica sands to:

$$I_D^2 = \frac{Q_{tn}}{constant} \quad (17)$$

Table 2 Shear wave velocities measured at the Los Angeles basin subarea (modified after [28])

Geologic unit	Shear wave velocity		
	Mean in m/s	SD	Range in m/s
Fine	200	20	150–270
Medium	230	30	195–285
Coarse	320	25	290–355
Very coarse	365	20	350–375

where I_D is expressed as a decimal. A constant of 350 is more reasonable for medium, clean, uncemented, unaged quartz sands that are about 1000 years old. The constant is closer to 300 for fine sands and closer to 400 for coarse sands as suggested by Robertson and Cabal [80]. According to Eq. 17, one can approximately estimate the ratio of Q_{tn} of coarse- and fine-grained soils at a constant I_D as $(400/300 \approx 1.33)$.

It appears clearly from the above discussion that V_s is correlated well with the void ratio, while N and q_c are more affected by I_D, and D_{50} has a significant effect on V_s as well as on (V_s/N) and (q_c/N) ratios with V_s and q_c being more sensitive to the change in D_{50} than N. The question arises as to whether V_s is more sensitive to grain size than q_c. The results of Menq [71], Bui [16], and the field data of [28] combined with Eq. 17 and the contribution of Karray et al. [52] as well as the more recent work by Hussien and Karray [39] all confirm that V_s is more sensitive to grain size than q_c in fine-to-course granular soils. However, [78] and (2012) supported by Andrus et al. [4] data from a wide range of soil types, including cohesive and non-cohesive materials, indicated that the V_s/q_c ratio decreases with the decrease in the SBTn index, I_c (i.e., the soil becomes more coarse grained as I_c is inversely proportional to main grain size, D_{50}). This aspect of soil behavior with respect to the effect of grain size (D_{50}) on V_{s1}/Q_{tn} trend will be detailed, analyzed, and discussed in the next section using a data set of different uncemented soils of Holocene age accumulated at various sites in North America, Europe, and Asia. These sites are carefully selected such that at each selected site, the V_{s1}/Q_{tn} correlation is derived from data of the same soundings with particle-size determination, and additional uncertainties induced by spatial variability are thus eliminated.

3 Forms of V_{s1}–Q_{tn} correlations

In the framework of developing an V_{s1}–Q_{tn} correlation, applicable to different uncemented relatively young Holocene-age granular soil deposits, a wide range of V_{s1} and Q_{tn} data with particle-size determination on different soil types at various sites in the USA, Canada, Norway, Italy, Ireland, Taiwan, and Hong Kong were collected, detailed, and analyzed. These data are then utilized in constructing a general correlation between $V_{s1}/Q_{tn}^{0.25}$ ratio and D_{50}.

All the used data are carefully selected from only sites with SCPT except in the case of Péribonka site where a significant Péribonka database was obtained from MMASW tests as well as CPT (1084 pairs). Karray and Lefebvre [50], however, have demonstrated that the MMASW test results are in accordance with the SCPT

performed at the Péribonka site. This issue has been later confirmed by Karray et al. [51] using Péribonka data before and after compaction.

At all sites, the total vertical stress, σ_v, is subtracted from q_t to obtain the net total cone resistance $(q_t - \sigma_v)$. The sets of V_s and $(q_t - \sigma_v)$ profiles are normalized for a 100-kPa effective vertical stress according to Eqs. 1 and 4, respectively, to obtain the normalized quantities V_{s1} and Q_{tn}. For all studied cases, the stress exponent, n in Eq. 4, although depends on the soil type, is selected at 0.5 as the data are rather biased toward sands and sandy soils. However, the effect of changing the exponent n on the $V_{s1}/Q_{tn}^{0.25} - D_{50}$ is also discussed.

In few cases, the q_t profiles show strong irregularities that are considered here as being associated not with the material density, but rather with contacts with coarse elements. Representative points have been defined on the profiles approximately every meter down, and the marked irregularities in the q_t profiles were neglected, as illustrated in Fig. 2. A value for V_s has been considered at the same elevation; each of the profile sets thus provides a number of representative points used to establish the correlations [52]. Summary of the used case histories is presented in Table 2, and more details of the test sites are given in the following subsections:

3.1 Péribonka dam site, Canada

The Péribonka dam, in northern Québec, Canada, is an embankment dam constructed on deposits found at the bottom of the river and generally constituted of well-graded gravelly sand to gravel. The sediments appear to be a fluvioglacial deposit formed during the last ice age 7800 to 9800 years ago [9]. An initial sub-rounded gravelly sand filling, generally 10–12 m in thickness, was dumped on the alluvial forming a platform at elevation 180 m. This filling and the foundation alluvium were then compacted prior to the installation of a plastic concrete diaphragm wall. Accordingly, the soils (fill and foundation) at the Péribonka site are of Holocene age, are uncemented, and are predominantly of quartz minerals with feldspar (quartzo-feldspathic) and an amount of ferromagnesium. The sandy materials encountered in Péribonka are rather well graded and coarser, with D_{50} mean value around 1.9 mm and a somewhat significant gravel portion. It should be noted here that centrifuge research work undertaken by many researchers (e.g., [10]) showed that when the cone diameter is greater than twenty times the mean particle diameter D_{50} of the soil (which is the case in Péribonka site and all other considered sites), the particle size has no practical impact on the measured penetration resistance.

The compaction by vibroflotation was monitored through CPTs and V_s, determined by MMASW tests. CPT
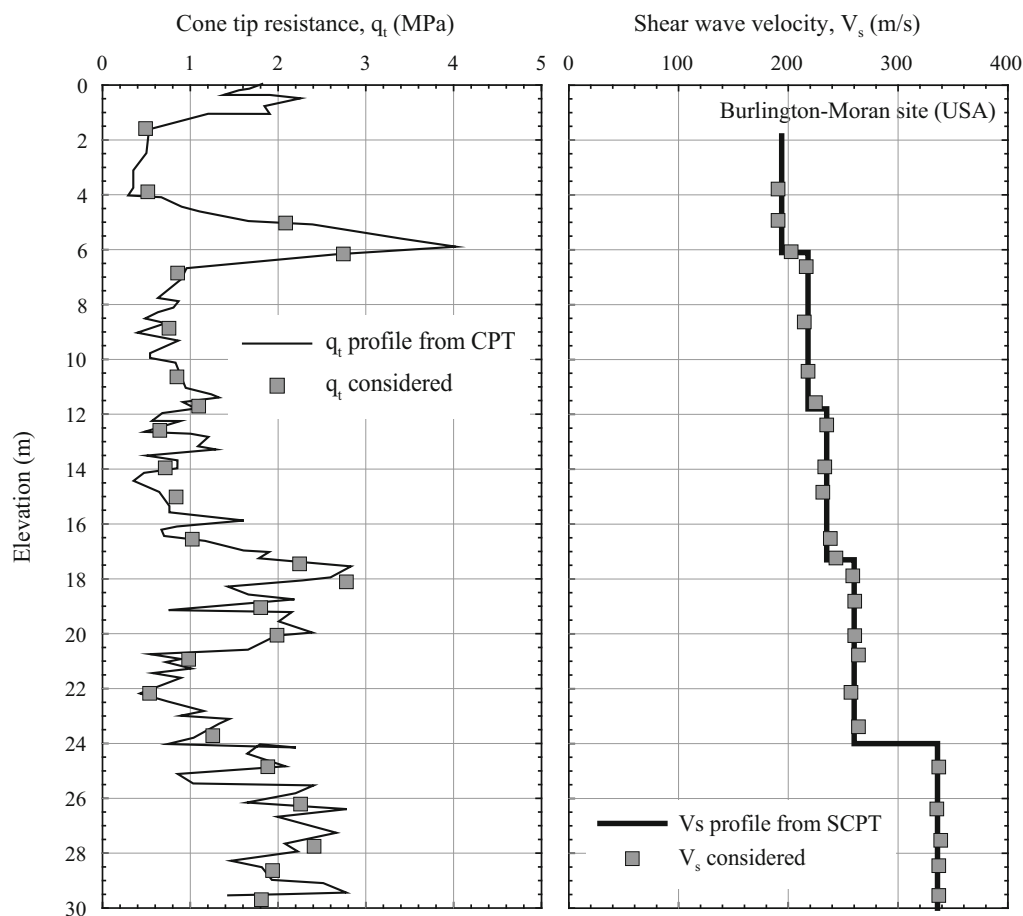
Fig. 2 Sample representative points defined in the V_s and q_t profiles at Burlington–Moran site (USA)

and MMASW testing programs were conducted prior to and following vibroflotation. The details of the MMASW procedure and V_s results at Péribonka dam are presented by Karray et al. [51]. More than 1000 CPT tests were performed, especially following compaction, so that a large number of direct comparisons could be made between q_c profiles and V_s profiles located close to one another. The detailed CPT tests results performed within a short distance of the MMASW sounding lines are presented by Karray and Lefebvre [50]. A total of 99 q_c profiles were compared one by one with the V_s profiles located within a short distance. The distance between the compared q_c and V_s profiles is less than 5 m in 62% of the cases and less than 7.5 m in 91% of cases [50].

3.2 CLK airport, Hong Kong

The Chek Lap Kok (CLK) airport is located on the northern coast of Lantau Island, Hong Kong. The CLK airport is being constructed on the 1248-hectare site of which 938 hectares is reclaimed land. The reclamation for the CLK airport included the placement of a substantial

volume of sand fill by various hydraulic placement techniques, which resulted in a wide range of as-placed densities of the sand fill. Hydraulic sand fills are very young, freshly deposited, waterborne sediments. They are usually characterized by low relative density, low strength, and high liquefaction potential, unless they are densified during or after placement. The sand is a uniformly graded to well-graded, rounded to sub-rounded, clean sand with an average specific gravity of 2.63. The fines content is generally less than 12%, with an average of 3%. The mean grain size, D_{50}, is about 1.0 mm, the average uniformity coefficient (D_{60}/D_{10}) is 4.5, and the average coefficient of curvature (C_c) is 0.9. The sand is comprised of 84–92% quartz, 5–10% plagioclase and alkali feldspars, 3–6% calcite and shells, and small percentages of other minor minerals such as magnetite, muscovite, biotite, and hematite and microfossils. V_s measurements were taken by seismic piezocone which involves a penetrating cone in which geophones are incorporated to detect a shear wave generated at the ground surface. The normalized shear wave velocity, V_{s1}, at CLK airport ranged from 200 to 280 m/s [59, 91].

3.3 Gioia Tauro, Italy

The test site is located in the harbor area of Gioia Tauro, in the southern part of Italy. Gioia Tauro lies on a flat plain, the origin of which was a depression, spreading along its length in an N–S direction from the Valley of Mèsima to the Massif of the Aspromonte and filled by continental sediments. This plain is prevalently constituted by granular saturated soils in the surficial layers (up to a depth ranging from 50 m to 70 m from the ground level) with an average D_{50} of about 1.0 mm. The V_{s1} and q_{c1N} data were determined, respectively, based on laboratory resonant column and CPTs calibration chamber tests and were found to be in the range of 200–300 m/s and 100–220, respectively [7, 26].

3.4 Holmen, Norway

Holmen is an island in the Drammen River just downstream from Drammen, Norway. Below a 2-m-thick sand fill, there is a very uniform sand layer extended to 22 m depth. This sand layer is very loose, medium to coarse grained with D_{50} of 0.49–0.90 mm and V_s of 120–210 m/s. Between 22 and 30 m, there is a fine- to medium-grained compact sand layer with D_{50} of 0.20–0.50 mm. The site was investigated in 1982 with the piezocone and later in 1985 with the seismic cone. Three repeated SCPTs were performed in 1985. The data are reported in [24]. The site is of interest because of its very uniform nature and the fact that comparative testing was possible. Tests with the UBC seismic cone at Holmen offered a good opportunity to verify the down-hole V_s measurement technique and compare results to cross-hole and surface wave techniques [32].

3.5 New York, USA

The test site is located within Brookhaven National Laboratory, in Upton, New York. During the period July 19 to 21, and August 16, 2006, four test borings and twelve cone penetrometer soundings were conducted. Shear wave velocity measurements were taken in four CPTs only at 3-m intervals. The CPT soundings penetrated to depths typically ranging from 16 to 30 m and were terminated at refusal or at a maximum depth of 30 m. Each of the borings encountered fill typically described as silty sand (SM), and the thickness ranged from 1.0 to 2.1 m. A thick layer of stratified sand, sand with silt, and sand with gravel with an average D_{50} of 0.45 m was encountered below the fill in all of the explorations. The sand is light brown to brown. SPT N-values ranged from about 15 bpf (medium dense) to greater than 50 bpf (very dense). The average corrected SPT N-value calculated from the CPTs within the upper

15 m was about 30 bpf. The CPTs detected some localized zones with equivalent N-values between 10 and 20 bpf. Shear wave velocity measurements indicate a uniform to slightly increasing shear wave velocity with depth. Velocities varied from 260 to 360 m/s. The average of 34 shear wave velocity tests in the four CPTs was 300 m/s [30].

3.6 Po River, Italy

The Po is a river that flows 652 km eastward across northern Italy. The Po River sand is a relatively thick deposit of clean to slightly silty sand that has been subjected to a great number of in situ tests, including SPT, CPT, CPMT, PMT, SBP, DMT, and Vs [15, 31, 44]. The sand is lightly overconsolidated due to groundwater fluctuations and aging with an average D_{50} of about 0.25 mm. The V_{s1} and q_{c1N} data were determined, respectively, based on laboratory resonant column and CPTs calibration chamber tests and were found to be in the range of 165–240 m/s and 57–250, respectively [7].

3.7 CANLEX project, Canada

In the context of studying the phenomenon of soil liquefaction, the Canadian geotechnical engineering community has conducted a major collaborative 5-year research project entitled the Canadian Liquefaction Experiment (CANLEX). The CANLEX project has involved the investigation of six sites in Western Canada, all of which contain relatively loose sand deposits. The investigations involved ground freezing and sampling as well as conventional sampling to obtain soil samples from each site. The sands at the CANLEX sites of Holocene age are essentially normally consolidated and appear to be uncemented and are composed primarily of quartz minerals with small amounts of feldspar and mica. These sands are uniformly graded with D_{50} of 0.16–0.25 mm and a fines content of generally less than 12%, with some less than 5% [85, 102].

Extensive in situ testing was performed at each site, and it consisted of the following: CPT, SPT, geophysical (gamma–gamma) logging, pressuremeter testing, and down-hole V_s measurements through SCPTs. The advantage of SCPT was that both the conventional CPT measurements and the V_s measurements were taken in the same sounding and allow for two independent in situ assessments of a given soil deposit at the same depth and spatial location. The CPT and V_s results for each of the six CANLEX sites were normalized with respect to the effective overburden stress. q_{c1N} was found to range from 20.4 to 73.8, F from 0.369 to 0.872%, and V_{s1} from 127.1 to 177.4 m/s [85, 102].

3.8 Chi-Chi, Taiwan

The case studies presented in this section are derived from sites located in the towns of Nantou, Yuanlin, and in the Chang-Bin industrial park in the central west Taiwan and were affected by soil liquefaction in the Chi-Chi earthquake. Two hundred and sixty-two CPT soundings conducted by Moh and associates [65] were collected from these areas, including 28 in Nantou, 201 in Yuanlin area, 30 in Chang-Bin, and 3 in an adjacent town (Donan). The geotechnical characteristics in these areas are derived from the CPT soundings. Typical subsurface conditions in each of the three areas, as revealed from CPT soundings, are briefly described in the subsections that follow [56]:

3.8.1 Site in Yuanlin (YL2)

Yuanlin (YL2) is one of the most severe liquefaction damage areas in the Chi-Chi earthquake. The CPT sounding at this site shows that q_c and f_s are generally low within 8.1 m below the ground surface. The average q_c is 2.57 MPa, and the average f_s is 19.62 kPa. The pore pressure and friction ratio suggest that the soil within the depth of 8.1 m is a loose sandy soil. Based on the grain size distribution curves, the soil is generally classified as SM with a FC of about 15% and an average D_{50} of 0.25 [56].

3.8.2 Site in Chang-Bin industrial park (LW-C1)

The Lunwei site in the Chang-Bin industrial park is in a reclaimed land by hydraulic fill. Extensive liquefaction and sand boiling phenomena were observed in this area in the Chi-Chi earthquake. The average q_c and f_s are 5.3 MPa and 25.8 kPa, respectively, from the ground surface to the depth of 3 m, where the soil is classified as loose to medium dense sand with D_{50} of 0.21 and average V_s of about 188 m/s. The next layer, between the depths of 3 and 7.6 m, is very loose sand with average V_s of about 123 m/s where the average q_c and f_s are 1.96 MPa and 6.9 kPa, respectively. The soil is classified as SP-SM with 8–10% of fines [56].

3.8.3 Site in Nantou (NT1)

The site in Nantou (NT1) consists of a shallow medium dense sand layer from the ground surface to a depth of 4 m with average Q_{tn} and f_s values that are 17.7–20.1 and 21.3 kPa, respectively. In the layer between 4 and 10 m, the average values of Q_{tn} and f_s are 25–90 and 80.4 kPa, respectively. A low shear wave velocity zone at the depth shallower than 4 m was measured, where V_{s1} is 128–146 m/s. V_{s1} at the depth between 4 and 8 m is about 156–214 m/s. The ejected sand at this site was found to

have an average D_{50} of 0.11 and a fines content of about 31–40%, and all soils at this site are classified as SM [56].

3.9 Wildlife, USA

The Wildlife site is located 3.2 km south of Cali patria in the Imperial Valley, California, USA. The Wildlife suffered liquefaction damage during the 1979 El Centro earthquake. Six CPT, nine DMT, and two SPT tests were conducted at this site. The site lies on the west side of the incised flood plain of the Alamo River. The stratigraphy at this site in the upper 12.0 m consists of horizontal layers of silts and sands with D_{50} of 0.15–0.25 mm, average V_{s1} of about 154–174 m/s, and Q_{tn} of 60–84 [32].

3.10 Heber Road, USA

The Heber Road site is located in the Imperial Valley of southern California at the north end of Heber Dunes County Park, approximately 20 km southeast of El Centro, between the Imperial Fault and the Alamo River. More details on the geographic location and geological features can be found elsewhere (e.g., [8, 12]). The site is of interest because of liquefaction-related damage caused by the El Centro earthquake 1979. To study the effects of the 1979 earthquake on the soil deposits located at the Heber Road site, extensive geotechnical investigation was carried out by Purdue University researchers in collaboration with the US Geological Survey between 1983 and 1985 along Heber Road, adjacent to an irrigation canal and the northern boundary of Heber Dunes County Park. This investigation included 20 CPT soundings and 23 flat dilatometers tests (DMT) soundings. Based on the in situ data, the upper 5 m of the soil profile at the Heber Road was found to consist of three different units of sand and silty sand. The unit referred to A_2 in [12] is of interest in this study. A_2 comprises a channel fill formed by dark brown, very loose, moderately sorted silty sand and fine sand with mean grain size, D_{50} of 0.10–0.12 mm, average V_{s1} of 116–206 m/s, and Q_{tn} of 13–51. The three units were formed by the fluvial activity in the relict channel during the late Holocene age (Bennett et al. l98 l; [12, 32]).

3.11 Alaska sand, USA

Alaska sand is angular sand obtained from a marine tailings deposit in the state of Alaska, USA. The deposit is from an old mine waste area and has been in a marine environment for up to 70 years. The stratigraphy of the soil profile at the test site consisted of about 15 m of silty sandy tailings material mixed with shell fragments. The mean grain size $D_{50} = 0.12$ mm, and the fines content was about 32% with a specific gravity of 2.90 and maximum and minimum void

ratio of 1.78 and 0.70, respectively. At the test site, data were used from two boreholes with SPT blow count values, as well as three SCPT profiles. The five investigation holes were all along a section line in order to analyze the soil profile for possible liquefaction. The field V_s and q_c data from the SCPT were in the range of 100–250 m/s and 1–8 MPa, respectively, for a vertical effective stress, σ'_v, from 10 to 250 kPa. σ'_v was calculated based on an estimated bulk soil density of 20 kN/m³ and with the water table just below the surface [22].

3.12 Venice lagoon, Italy

Venice lagoon soils are generally composed of a predominantly silt fraction combined with sand and/or clay forming an erratic inter-bedding of various sediments, whose basic mineralogical characteristics vary narrowly, as a result of similar geological origins and common depositional environment [37]. The deposits forming the upper 50–60 m below mean sea level are characterized by a complex system of inter-bedded sands, silts, and silty clays, deposited during the last glacial period of the Pleistocene Epoch when the rivers transported fluvial material from the Alpine ice fields. The Holocene Epoch is only responsible for the shallowest lagoon deposits up to 10–15 m below ground level. Comprehensive geotechnical studies were carried out to characterize the Venetian soils in the context of a huge project that was undertaken at the beginning of the 1980s under the directive of Italian Government to protect the city of Venice and the surrounding lagoon against the recurrent flooding. Two typical test sites in the lagoon—the Malamocco Test Site (MTS) and the Treporti Test Site (TTS)—were selected for the mechanical soil characterization and for a site-specific calibration of the most widely used geotechnical investigation tools [93]. The main geological and geotechnical features of the lagoon sediments at these two sites are briefly described in the subsections that follow:

3.12.1 Malamocco test site (MTS)

A series of investigations that included boreholes, piezocone (CPTu), dilatometer (DMT), self-boring pressuremeter (SBPM), and cross-hole tests (CHT) were performed at the first site located at the Malamocco inlet [19, 20]. Continuous coring was performed along two contiguous verticals using double-piston samplers, a standard 10-cm-diameter sampler, and a larger one with diameter of 20 cm. Freezing technique was used in sandy layers. The main grain size of the soil deposit, D_{50}, was 0.072 mm. The field V_{s1} and Q_{tn} data from in situ tests were in the range of 183–273 m/s and 34.5–128, respectively [20, 93].

3.12.2 Treporti test site (TTS)

The Treporti Test Site (TTS) is located at the inner border of the lagoon. Boreholes with undisturbed sampling, traditional CPT_U and DMT, seismic $SCPT_U$ and SDMT were employed to characterize soil profile and estimate the soil properties. The silty deposits of the Venetian lagoon area are largely recognized as the most well-studied silt materials in the world [99]. For this reason, three sets of data were considered in the current study. These sets of data are termed in Table 2, Treporti I, Treporti II, and Treporti III. The main grain size of the Treporti I, D_{50}, was 0.071 mm, and field V_{s1} and Q_{tn} data from in situ tests were in the range of 157–253 m/s and 11.7–117, respectively [92, 93]. For Treporti II, D_{50} was 0.035 mm, and field V_{s1} and Q_{tn} data from in situ tests were in the range of 154.8–198.2 m/s and 6.3–22.5, respectively. D_{50} of Treporti III was 0.14 mm, and field V_{s1} and Q_{tn} data from in situ tests were in the range of 143.6–303.6 m/s and 34–128, respectively [99].

3.13 Providence, Rhode Island, USA

A geotechnical site investigation was performed at the test site in Providence, Rhode Island, USA. The site consists of approximately 4 to 10 m of sand and gravel fill underlain by a thick layer of non-plastic silt. The silt was deposited as glacial lake sediments during the last glacial retreat and is therefore characterized by seasonal varves. Seismic cone penetration tests were performed with continuous measurements of tip resistance, sleeve resistance, and pore-water pressure, as well as shear wave velocity measurements at 1-meter intervals. Grain size analyses of bulk samples indicate that the silt is composed of about 95 percent fines (< 0.075 mm). The main grain size of the soil deposit, D_{50}, was 0.033 mm. The field V_{s1} and Q_{tn} data from in situ tests were in the range of 174–217 m/s and 17.9–48.5, respectively [13].

3.14 Foynes, Ireland

The test site at Foynes, beside the Shannon Estuary in the West of Ireland, is adjacent to a harbor access road that was constructed in 1999. The road crosses a large pocket of estuarine material that is relatively homogeneous in nature with predominantly gray marine silt. The deposit is up to 14 m deep, and the water table is close to ground level. The organic content of the soil is very low with an average value of roughly 2%. Particle-size distribution test was performed on samples extracted from shallow depth of 4 m and deep depth of 8 m. The soil is generally uniform graded from fine sand/coarse silt to clay. The upper samples are coarser than the lower samples. Sand content ranges

between 5 to 15% for shallow samples and 2% for deep samples. The main grain size of the soil deposit, D_{50}, was 0.022 mm. The site investigation program consisted of two CPTu tests and one ball test 5 m apart. Two SDMT tests were completed within 1.5 m of each other 5 m of probe tests. Large Q_{tn} peaks between 1.5 and 3.5 m are evident in the upper layer; Q_{tn} ranges from 11.7 to 15.5 due to a stiff layer. Below 3.5 m, Q_{tn} of 4.9–9.9 MPa is evident. Measurements of V_s show two different V_{s1} values, the first range is roughly 150–172 m/s from 1.5 to 3.5 m, and the second range is 144–167 m/s from 3.5 to 13.2 m [17].

4 Influence of D_{50} on V_{s1}–Q_{tn} correlations

Based on the wide range of data set presented above, a possible statistical trend between $V_{s1}/Q_{tn}^{0.25}$ ratio and D_{50} is examined, in an attempt to develop a global approach, valid for different uncemented, Holocene-age granular soils. Data from the 19 sites described in the previous sections in conjunction with centrifuge data from [25] as well as other data calculated from liquefaction charts proposed by Andrus and Stokoe [2] and [85] are simply plotted in Fig. 3 in terms of $V_{s1}/Q_{tn}^{0.25}$ ratio as a function of D_{50} ranging from 0.02 to 2.0 mm. The 95% confidence intervals are also shown in Fig. 3. The confidence intervals are used to show the proportion of points that may be expected to contain the true mean, and the end points of the confidence interval are referred to as the confidence limits. The exponential parameter of Q_{tn}-value is selected at 0.25 close to those suggested by Robertson et al. [84], Fear and Robertson [27], Wride et al. [102], and Karray et al. [52] (from 0.23 to 0.25) and presented in Table 1. These relationships have furthermore the advantage of having been established for relatively uncemented young sand deposits (Holocene age), such as most of the field cases considered in this study. The results in Fig. 3 exhibit some features that warrant explanation:

1. As expected, the effective mean diameter, D_{50}, of the soil has a significant impact on the $V_{s1}/Q_{tn}^{0.25}$ ratio.
2. $V_{s1}/Q_{tn}^{0.25}$ correlation shows different trends with respect to particle grain sizes. For soils with $D_{50} < 0.2$ mm, the $V_{s1}/Q_{tn}^{0.25}$ ratio undergoes a substantial decrease with the increase in the mean effective diameter. Considering the D_{50} effect, the relationship between V_{s1} and Q_{tn} in this range of particle size can therefore be expressed as:

$$\frac{V_{s1}}{Q_{tn}^{0.25}} = 43.7/D_{50}^{0.215} \qquad (18)$$

3. The above trend is totally reversed with further increase in D_{50} of the soil ($D_{50} > 0.2$ mm), and the $V_{s1}/Q_{tn}^{0.25}$ ratio can be expressed as:

$$\frac{V_{s1}}{Q_{tn}^{0.25}} = 71D_{50}^{0.1} \qquad (19)$$

In Eqs. 18 and 19, V_{s1} is expressed in m/s and D_{50} in mm.

4. These results confirm earlier results (e.g., [52, 99]) that stressed on the use of different correlations with different soil types and emphasize the need at least to impose particle-size limits on the validity of the majority of the available empirical formulations.

It is fair to mention here that the reversing trend of $V_{s1}/Q_{tn}^{0.25}$ ratio with respect to D_{50}, presented in Fig. 3, is not totally unknown to the geotechnical community. Some researchers reported similar soil behavior with respect to grain size. For example, [74], based on controlled experimental tests, demonstrated that the ratio V_s/N for cohesionless soils is 67.79 for fine sand, 63.94 for medium sand, 66.68 for coarse sand, 71.52 for gravelly sand, and 92.28 for gravel. These results are schematically portrayed in Fig. 4a. The experimental data of Suzuki et al. [96] (Fig. 4b) indicate clearly that the V_{s1}–Q_{tn} data exhibit different trends with respect to grain sizes. Moreover, [40] in the context of developing a procedure for the quantitative determination of some soil parameters to be used in the estimation of soil liquefaction potential, reported that the cyclic stress ratio (CSR) experiences a substantial decrease with the increase in D_{50} and reaches its minimum value at ($D_{50} \approx 0.2$ mm). With further increase in D_{50}, CSR gradually increases.

The potential reason why the reversing trend of $V_{s1}/Q_{tn}^{0.25}$ ratio with respect to D_{50} is not previously determined is that the current correlations (Eqs. 18, 19) as well as [74] and [52] utilize directly the main grain size, D_{50}, as a direct measurement of the soil grain size, while in constructing other correlations such as those of Robertson [79] and Andrus et al. [4], there are no physical determination of the soil grain sizes in the field and the grain size is accessed indirectly through the use of I_c. In fact, I_c cannot be expected to provide accurate predictions of soil grain size, but provide a guide to the mechanical characteristics (strength and stiffness) as stated plainly by Robertson [80]. In addition, I_c calculated from Eq. 8 includes both friction ratio, % F and Q_{tn}, and a correlation between $V_{s1}/Q_{tn}^{0.25}$ and I_c is not expected therefore to provide a clear trend as one of the correlative parameters (Q_{tn}) is incorporated in both sides of the correlation.

Besides, the current study data (i.e., V_{s1}, Q_{tn}, and D_{50}) are treated globally (i.e., site by site or layer by layer). This method of data treatment eliminates the variability induced by the nature of the q_t measurement significantly affected by the locale variation in soil unlike shear wave velocity
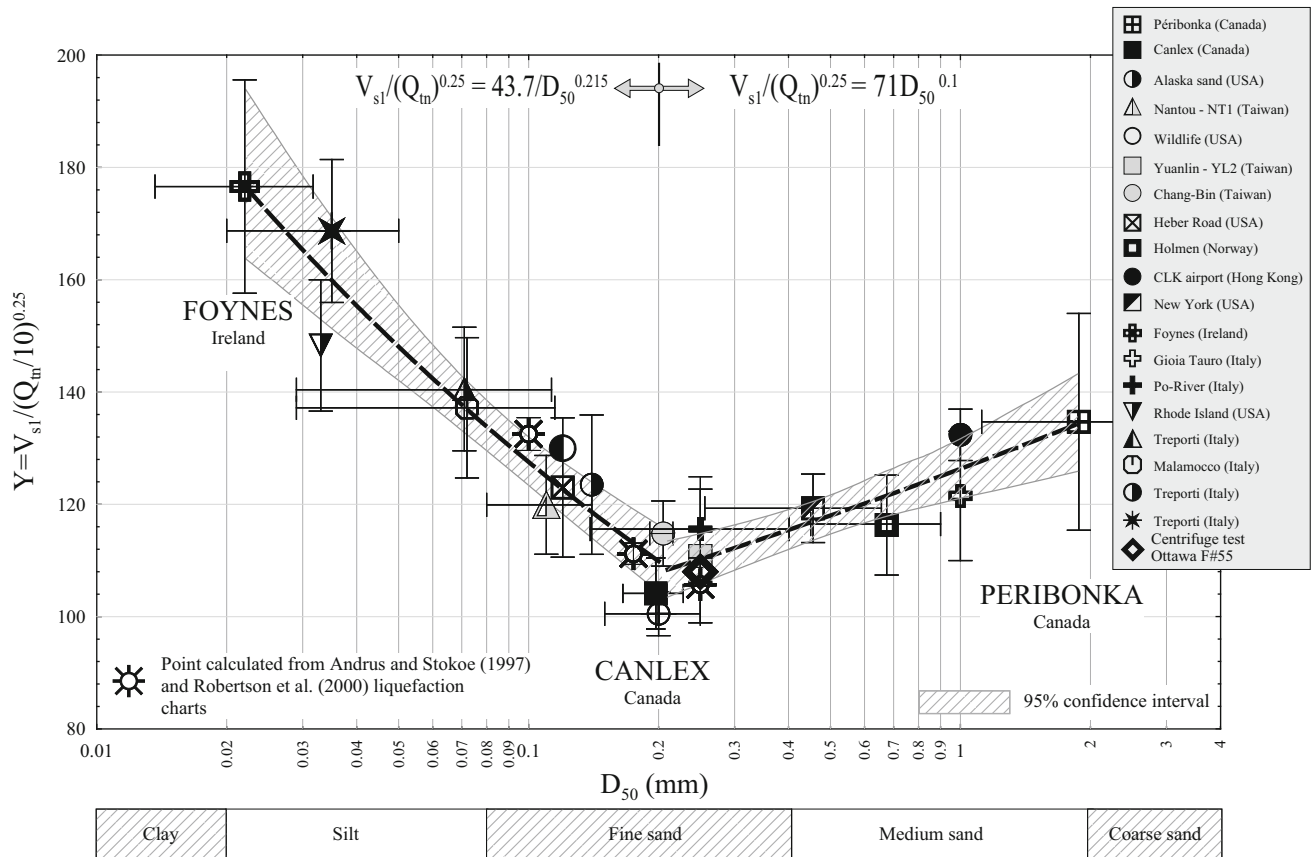
Fig. 3 Variation of $Y = V_{s1}/(Q_{tn}/10)^{0.25}$ as a function of the D_{50} values for uncemented, Holocene-age soils

that represents a certain volume of soil. Most of the V_{s1}–Q_{tn} correlations found in the literature were constructed strictly point by point without eliminating the noisy data associated with nature of the cone resistance measurement.

In fact, the reversed trend in Figs. 3 may be attributed to the difference in the soil compressibility. In developing their V_{s1}–q_{c1} correlations, although used a constant exponent value of 0.25 for both compressible (Alaska sand, $D_{50} = 0.12$ mm) and incompressible (Ottawa sand $D_{50} = 0.34$ mm), [27] suggested different correlative constants to account for soil compressibility. Fear and Robertson [27] further stated that soil compressibility will not significantly affect the measured V_s, since shear waves do not compress the soil, but it can greatly affect CPT penetration resistance, since the more compressible the soil, the lower the penetration resistance, even at the same relative density. In fact, combining the data of Fear and Robertson [27] with field data presented in Fig. 3 suggests that around D_{50} of 0.2 mm, soil behavior changes with respect to compressibility. In other words, D_{50} is probably a borderline between compressible and incompressible soils. The reversed trend in Fig. 3 may be attributed also to the difference in the sensitivities of the parameters (V_{s1} and Q_{tn}) to grain sizes as well as the drainage conditions of the soils. In other words,

standard CPT tests in soils with $D_{50} < 0.2$ mm (i.e., silt or silty sand) may be partially drained producing a relatively lower penetration resistance compared to the drained tests of the same soil. It is worth to note here that the drained CPT tests can be performed on silt or silty sand soils by lowering the penetration rate as the tests done by Krage and DeJong (2014) to investigate the effect of the penetration rate on the measured penetration resistance of natural deposits of sands with fines at three different sites, namely Kornbloom, Lenordini, and Granite sites. Table 4 presents some of the Krage and DeJong results concerning the used penetration rate and the corresponding penetration resistance as well as the measured shear wave velocity. The data presented in Table 4 infer that lowering the penetration rate of soils having $D_{50} < 0.2$ mm from the standard rate (≈ 20.2 mm/s) to a rate of about 0.2 mm/s will significantly increase the normalized penetration resistance and the percentage of increase reaches 48%. On the other hand, the normalized shear wave velocity is not affected by draining conditions (i.e., lowering the penetration rate) as it is an effective stress parameter [39]. This leads us to say that for partially drained soils, the $V_{s1}/Q_{tn}^{0.25}$ ratio decreases as the soil becomes drained (i.e., the increase in D_{50}). It should also worth to mention that the borderline between partially and fully

drained soils suggested by many researchers and plotted on the well-known q_{t1N}-F % charts coincides with $I_c = 2$ ($D_{50} = 0.2$ mm) as it is schematically shown in Fig. 5. Table 4 illustrates also that the penetration rate has no practical effect on the penetration resistance and consequently the $V_{s1}/Q_{tn}^{0.25}$ ratio of the soil at Granite site ($D_{50} = 0.3$ mm > 0.2 mm) as the CPT tests in this soil are almost drained.

The increase in $V_{s1}/Q_{tn}^{0.25}$ ratio with increasing D_{50} for fully drained soils ($D_{50} > 0.2$ mm), presented in Fig. 3, can be also visualized referring to the results of Menq [71], Bui [16], and the field data of [28] combined with Eq. 17 and the contribution of Karray et al. [52] as well as the more recent work by [39] that confirm that V_s is more sensitive to grain size than q_c in fine-to-course granular soils. More specifically, V_s of granular soils increases faster than penetration resistance as grain size increases.

A matter of concern with the proposed $V_{s1}/Q_{tn}^{0.25}$–D_{50} formulations (Eqs. 18, 19) is that the same stress normalization is adopted in all studied cases. In other words, V_s and q_t profiles are normalized with respect to the effective vertical stress, σ_v', according to Eqs. 1 and 4 with stress exponents of 0.25 and 0.5, respectively. In fact, experimental work undertaken by many researchers with variety of soils has suggested that V_s increases in an exponential manner with σ_v' and a stress exponent vary from 0.20 to 0.30 (e.g., [36, 46, 61, 72]) among others, and a practical value of 0.25 was proposed by many researchers [72]. The stress exponent, n, in Eq. 4 is typically equal to 1.0 for soil classification in clay-type soils ($I_c > 2.6$) and 0.5 for sandy-type soils ($I_c < 2.6$). The value of n is selected at 0.5 as the data are rather biased toward sands and sandy soils. Moreover, the effect of changing the exponent n on the $V_{s1}/Q_{tn}^{0.25}$–D_{50} in soils with $D_{50} < 0.2$ mm is discussed in Fig. 6 and Table 5. The data are re-analyzed considering three different values of n (0.5, 0.75, and 1.0). Figure 6 demonstrates that the change in the n value, although changes slightly the $V_{s1}/Q_{tn}^{0.25}$–D_{50} relationship, does not appear to affect the correlation trend. Table 5 also illustrates that the probable error is affected by the adopted n value and the minimum error is generally associated with $n = 0.5$. Table 5 also examines the error stemming from adopting the dimensionless total penetration resistance, q_{t1N}, instead of Q_{tn}, where q_{t1N} can be estimated as:

$$q_{t1N} = \left(\frac{q_t}{P_a}\right) \cdot \left(\frac{P_a}{\sigma_v'}\right)^n \tag{20}$$

Table 5 shows that the associated error is within 5%.

To be compared directly with the relationships proposed by [4], all the data from the aforementioned sites as well as [96] experimental investigation are re-plotted in Fig. 6 in terms of $V_{s1}/q_{t1N}^{0.411}$ ratio as a function of the Soil Behavior Type Index SBT (I_c) for a range of soil types
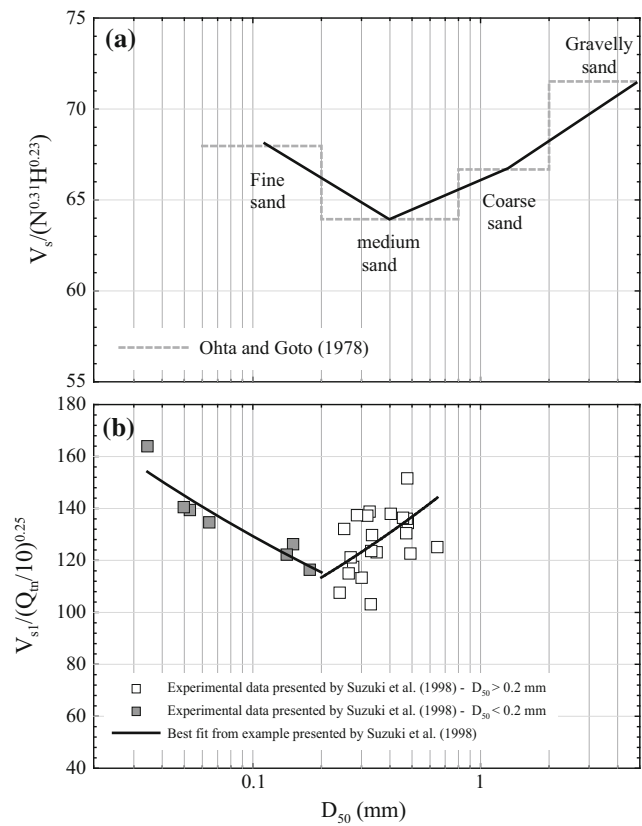

Fig. 4 Influence of the grain size on soil behavior observed by: **a** [74] and **b** [96]

($1.0 < I_c < 3.12$). I_c values are computed from D_{50} following the relationship suggested by Karray et al. [52]. The exponential parameter of q_{t1N}-value is selected at 0.411 as suggested by Andrus et al. [4] (Table 1). The $V_{s1}/q_{t1N}^{0.411}$-I_c correlation proposed by Andrus et al. [4] is also portrayed in Fig. 6 with its confidence intervals. Although almost all the field data collapse onto the range given by Andrus et al. [4] as shown in Fig. 7, the correlation proposed by Andrus et al. [4] tends to predict $V_{s1}/q_{t1N}^{0.411}$ values somewhat lower than the field data. It may be that the proposed relationship by Andrus et al. [4] using wide range of soil types and grain sizes may not have been well constrained as it simply averaged the data from fine- and coarse-grained soils which appears to be not reasonable as fine- and coarse-grained soils generally follow different trends as presented in Fig. 3. Divisions of data among different soil types (relative grain sizes) would improve the accuracy of correlative equations. For $I_c < 2.0$ ($D_{50} > 0.2$ mm), $V_{s1}/q_{t1N}^{0.411}$ can be expressed as:

$$\frac{V_{s1}}{q_{t1N}^{0.411}} = 51.1 I_c^{-0.737} \tag{21}$$

and for $I_c > 2.0$ ($D_{50} < 0.2$ mm), $V_{s1}/q_{t1N}^{0.411}$ can be written as:
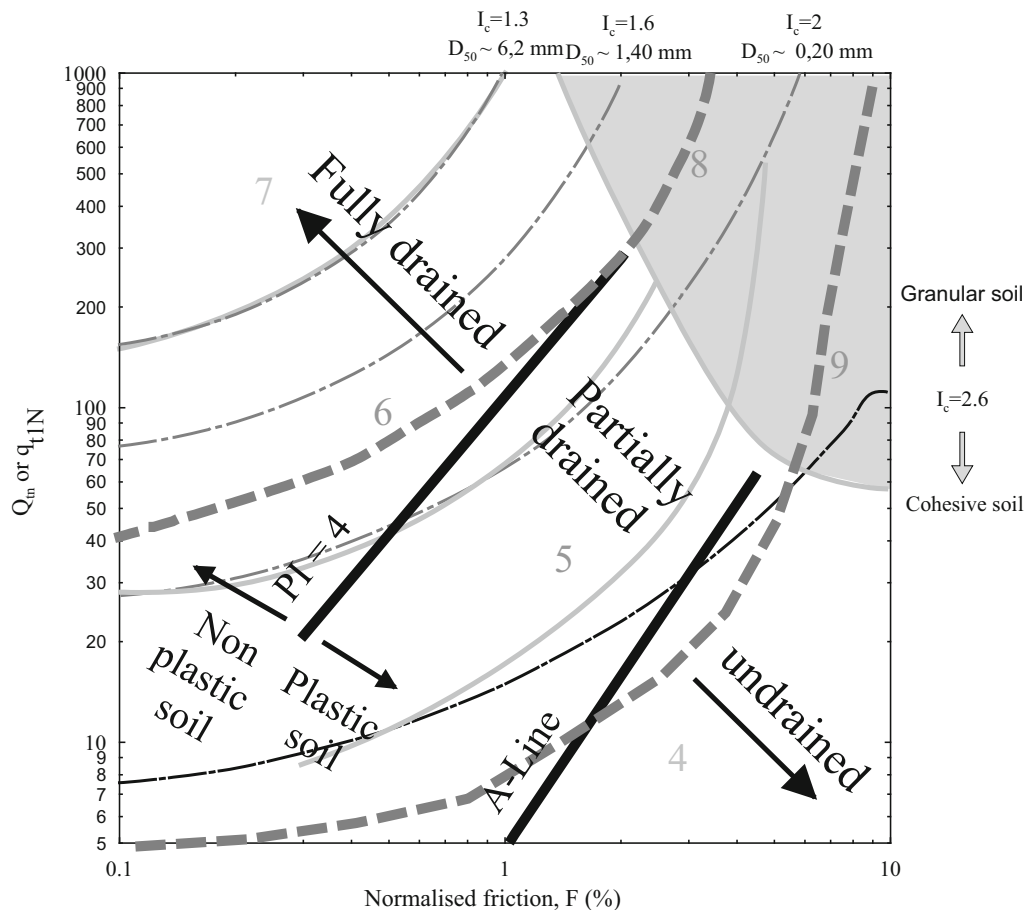
Fig. 5 Contours of D_{50} on q_{t1N} or Q_{tn}-$F\%$ charts. The plasticity limits are reported from Cetin and Ozan (2009). The drainage condition limits are reported from [43]. The values of D_{50} are estimated from Ic using equation proposed by Karray et al. [52]

$$\frac{V_{s1}}{q_{t1N}^{0.411}} = 11.94 I_c^{1.45} \tag{22}$$

5 Applicability of the proposed V_{s1}–Q_{tn} formulations

5.1 Comparison with laboratory measurements of V_s

The validity of the proposed V_{s1}–Q_{tn} correlations (Eqs. 18, 19) is assessed through comparisons with reliable experimental V_{s1} measurements available in the literature. Figures 8, 9 and 10 compare V_{s1}–e relationships measured in the laboratory with those predicted using Eqs. 18 and 19. The corresponding V_{s1}–e curves calculated from Andrus et al. [4] correlation given in Table 1 are also plotted in Figs. 8, 9 and 10 for comparison. In particular, Fig. 8 shows a comparison with the data reported by [91] through bender element (BE) tests on CLK sand ($D_{50} = 1.0$ mm), while Fig. 9 shows a comparison with those reported by Cunning et al. [22] based

on BE tests on Syncrude sand ($D_{50} = 0.17$ mm). Figure 10 shows a comparison with the data reported by Kokusho and Yoshida [55] through BE tests on TS sand ($D_{50} = 0.34$ mm). In Figs. 8, 9 and 10, the corrected normalized standard penetration test blow count, $(N_1)_{60}$, variation with e is first evaluated based on the correlation (Eq. 12) proposed by Kulhawy and Mayne [58]. It should be noted here that the minimum value of $(N_1)_{60}$ is selected at 2 for very loose state of soil ($I_D \approx 0$). The minimum and maximum limits of the corresponding normalized cone penetration resistances, q_{c1N}, are then estimated based on Eqs. 14 and 15, respectively. Following the recommendation of Robertson [79] and considering a maximum error within 5% (Table 3), Q_{tn} can be essentially considered equal to q_{c1N} for sandy soils. Depending on the value of the effective mean diameter, Eq. 18 ($D_{50} < 0.2$ mm) or Eq 19 ($D_{50} > 0.2$ mm) is then utilized to calculate the upper and lower limits of V_{s1}–e variations presented in Figs. 8, 9 and 10. Similar procedure is used to plot the upper and lower limits of V_{s1}–e variations based on [4] correlation by replacing Eqs. 18 or 19, depending on D_{50}, with the equation suggested by Andrus
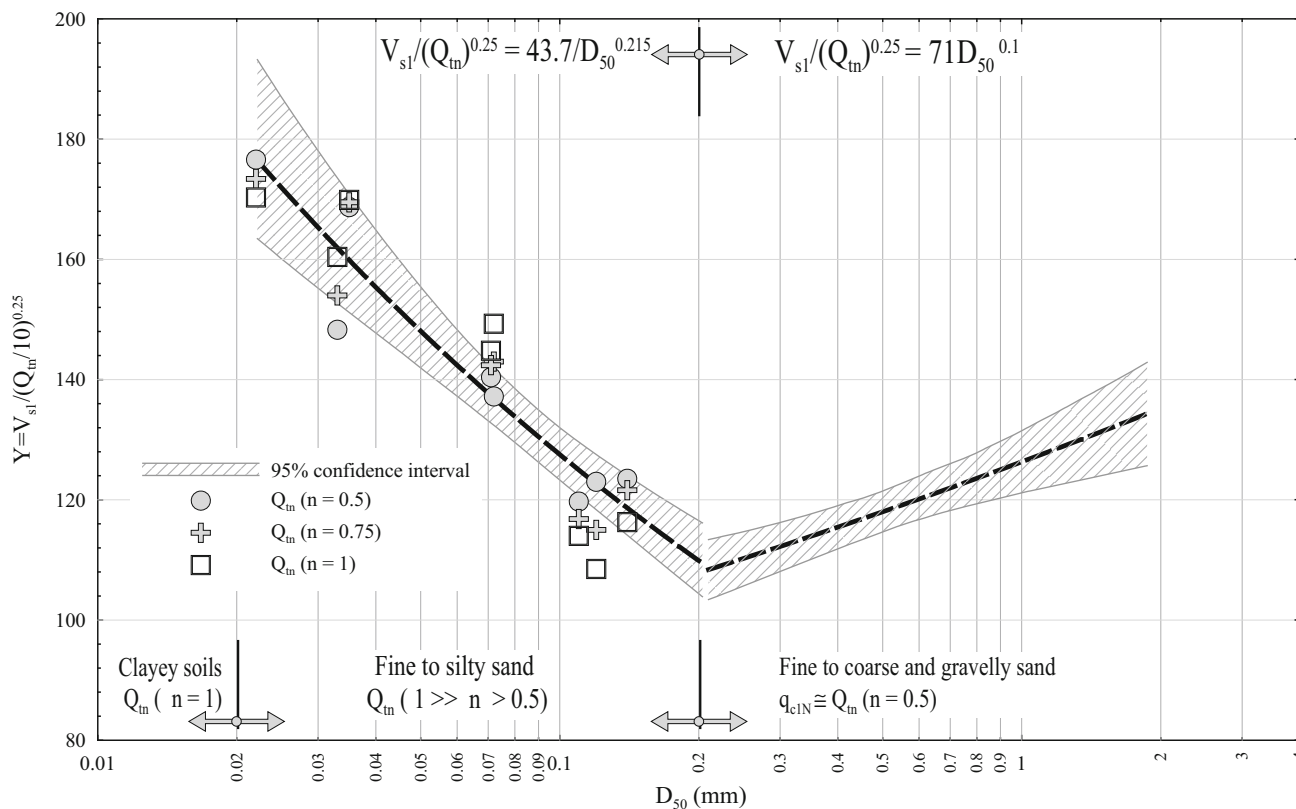
Fig. 6 Effect of the stress exponent, n, on V_{s1}–Q_{tn} correlations for relatively fine-grained soils ($D_{50} < 0.2$ mm)

et al. [4] (Table 1). Based on the comparative results shown in Figs. 8–10, the following trends should be highlighted:

1. In contrast to the correlation proposed by Andrus et al. [4] that gives up to a 225 m/s variation of V_{s1} between the loosest and the densest state of the soil, experimental and computed V_{s1} variations using Eqs. 18 and 19, at the same grain size, collapse onto a relatively narrower range. Similar note is reported earlier by Karray et al. [51] and verified by Ishibashi et al. [39] based on laboratory and field measurements of shear wave velocities of a wide range of uncemented soils. These results also confirm that the use of a correlative exponent of 0.25 would predict satisfactorily the variation of V_{s1} between the loosest and the densest state of the soil.

2. For CLK airport sand ($D_{50} = 1$ mm) [91], Fig. 8 shows that Andrus correlation greatly underestimated the normalized shear wave velocity of the CLK sand, especially at its loose state. In contrast, the use of Eq. 19 provided improved V_{s1}–e curves that agreed well with the experimental test results.

3. For Syncrude sand ($D_{50} = 0.17$ mm) [22], Fig. 9 indicates that the calculated V_{s1}–e curve based on the current correlation (Eq. 18) agreed well with the

measured data, but the calculated results based on [4] correlation generally underestimated the V_{s1} values.

4. For TS sand ($D_{50} = 0.34$ mm) [55], Fig. 10 shows that the predicted V_{s1}–e curve based on Eq. 19 agreed well with the measured data. In contrast, the predicted results based on [4] correlation generally overestimated the V_{s1} values of the TS sand at its densest state and underestimated them at the loosest state.

The data of BE tests on TS sand provided by Kokusho and Yoshida [55] are utilized in this section to further assess the validity of Eqs. 18 and 19. For different grain sizes in the range (0.15 mm $< D_{50} < 7.3$ mm), test results on TS sand [55] in terms of V_{s1}–e variations are compared to the $V_{s1\text{-min}}$ and $V_{s1\text{-max}}$ variations with e computed from the current study and those predicted by Andrus et al. [4] as well as [78] (Table 1) in Fig. 11a and b, respectively. To plot Fig. 11a and b, the maximum normalized standard penetration test blow count, $N_{1\text{max}}$, is first evaluated based on the effective mean diameter, D_{50}, from Eq. 12 assuming $I_D = 100\%$, while $N_{1\text{min}}$ is selected at 2.0. The minimum and maximum limits of the corresponding normalized cone penetration resistances, q_{c1N}, are then estimated based on Eqs. 14 and 15, respectively. Figure 11a illustrates that correlations proposed in the current study predict satisfactorily the variation of both $V_{s1\text{-max}}$ and $V_{s1\text{-min}}$ with e for
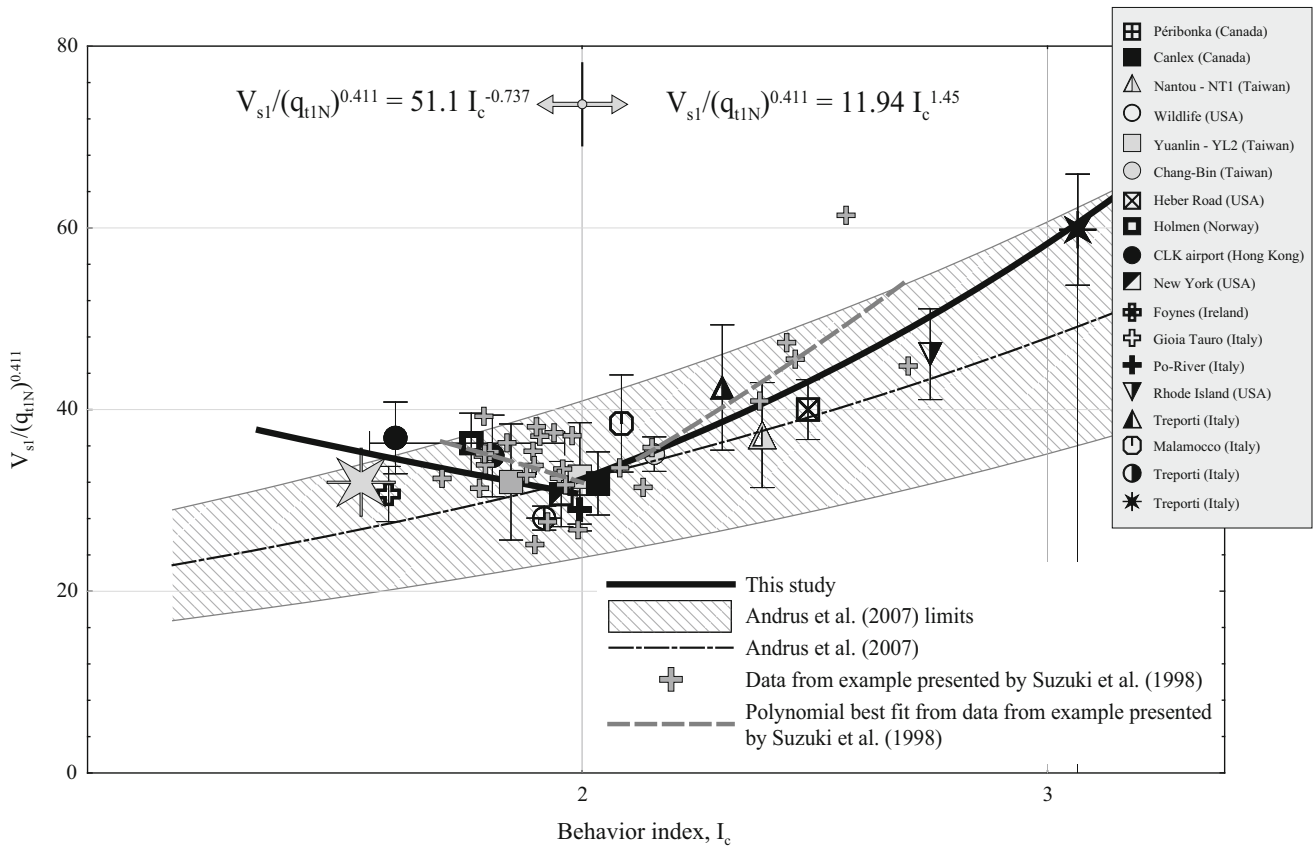
Fig. 7 Comparison between test data from the 19 sites in term of $V_{s1}/q_{t1N}^{0.411}$-I_c relationship with [4] correlation
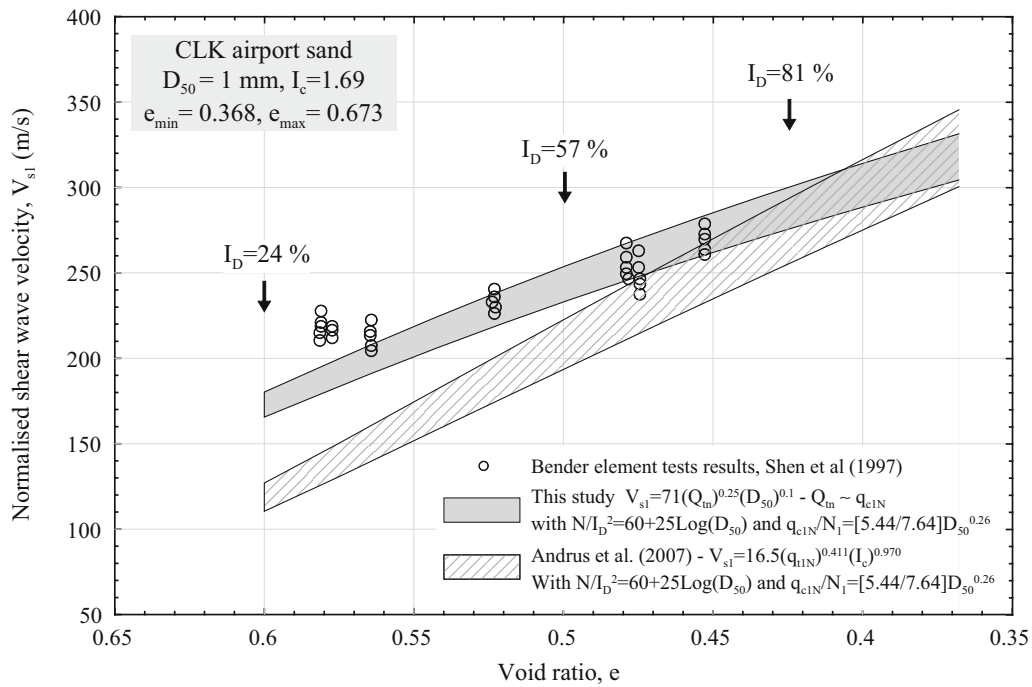

Fig. 8 Comparison between CLK airport sand test results [91] with $D_{50} = 1$ mm with those predicted by Eq. 19 and [4] correlation
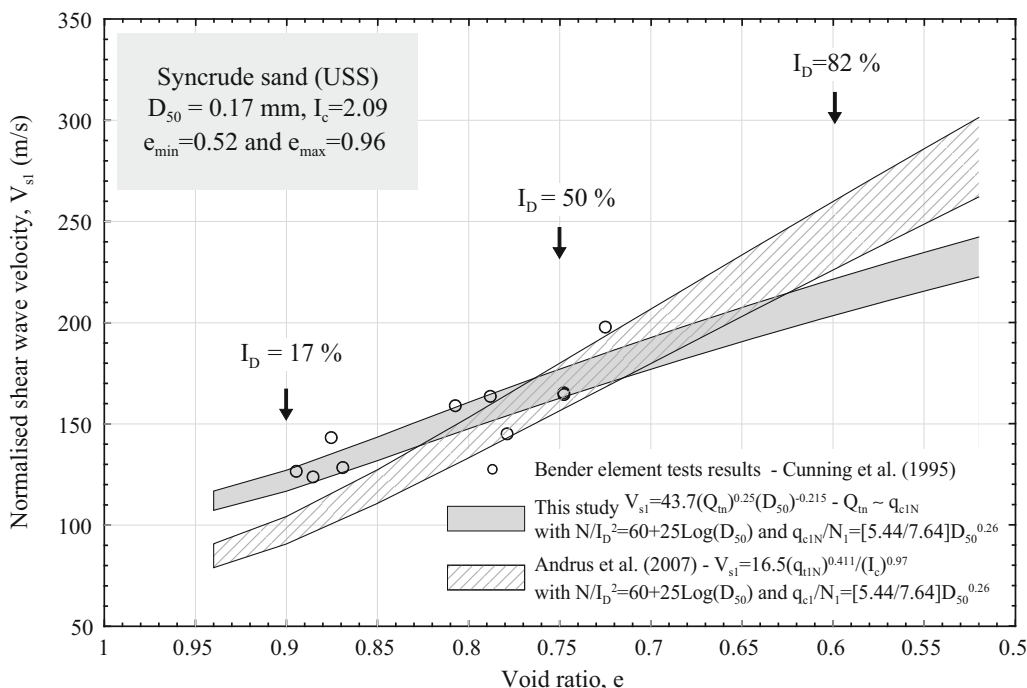
Fig. 9 Comparison between Syncrude sand test results [22] with D_{50} = 0.17 mm with those predicted by Eq. 18 and [4] correlation

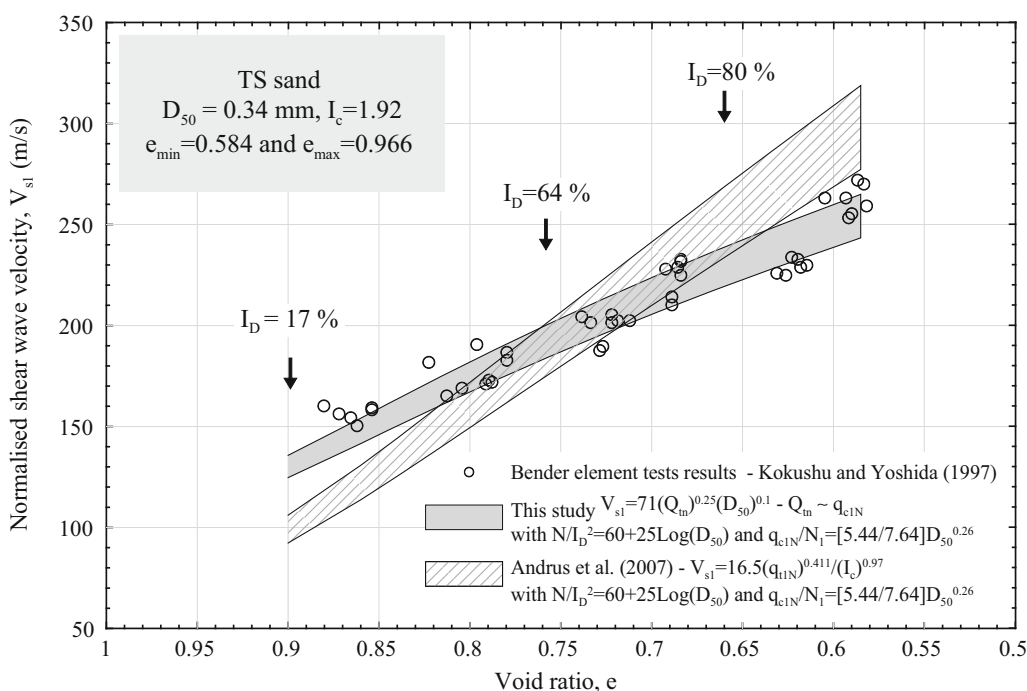**Fig. 10** Comparison between TS sand test results [55] with D_{50} = 0.34 mm with those predicted by Eq. 19 and [4] correlation

the range of grain sizes presented in the figure. In contrast, Fig. 11b shows that the variation of e has relatively little influence on V_{s1-min} and V_{s1-max} values according to [4] and [78]. Moreover, the correlations proposed by Andrus et al. [4] and Robertson [78] shown in Fig. 11b tend to predict, respectively, V_{s1-min} and V_{s1-max} values somewhat lower

and higher than the measured data. In other words, [4] and [78] correlations give up to a 300 m/s-variation of V_{s1} between the loosest and the densest state of the TS sand which appears to be different from that observed in the original data of tests performed by Kokusho and Yoshida [55] or those discussed by Hussien and Karray [39].

Table 3 Summary of studied cases used in developing V_{s1}–Q_{tn} correlations

Test site	D_{50} (mm)	I_c	Nb. of data pairs	Soil description	Mineralogy	Angularity	Geologic age	$V_{s1}/Q_{tn}^{0.25}$	Author(s)	Country	q_t or q_c (MPa) (q-rang) [depth]	V_s method
Péribonka dam	1.88 (0.76)	1.56	1084	Gravelly coarse sand	Quartzo-feldspathic with ferromagnesium	Sub-rounded to sub-angular	Holocene	134.7 (19.3)	Karray et al. [51]	Canada	Uncorrected, q_c	MMASW
CLK airport	1.0	1.68*	4	Marine sand	Quartz, plagioclase and alkali feldspars	Rounded to sub-rounded	Very young	130.1 (5.9)	Shen et al. [91]	Hong Kong	n.d.	SCPT
Gioia Tauro	1.0	1.68*	19	Silica sand	n/a	n/a	Very young	121.47 (11.44)	Baldi et al. [7]	Italy	n.d.	SCPT
Holmen	0.675 (0.225)	1.816 (0.154)	20	Very loose, medium to coarse sand	Quartz, K-feldspar, plagioclase, and amphibole	Rounded to sub-angular	Holocene	116.3 (8.9)	Gillespie [32]	Norway	Uncorrected, q_c (2.2–7.6) [2.6–19.6]	SCPT
New York	0.456 (0.2)	1.964 (0.077)	23	Sand with gravel and silt	n/a	n/a	n/a	118.46 (5.74)	GEI [30]	USA	Corrected, q_t (8.7–35) [4.2–28.6]	SCPT
Po River	0.25 (0.1)	1.996*	92	Silica sand	n/a	n/a	Very young	115.7 (9.3)	Baldi et al. [7]	Italy	n.d	SCPT
CANLEX project	0.197 (0.0314)	2.028 (0.22)	n/a	Fine sand	Quartz with small amounts of feldspar and mica	Sub-rounded to sub-angular	Holocene	104.65 (6.72)	Wride et al. [102]	Canada	Uncorrected, q_c (n.d.)[n.d.]	SCPT
Yuanlin	0.25	1.88 (0.32)	11	Silty sand	n/a	n/a	n/a	110.7 (11.9)	Kuet et al. [56]	Taiwan	Uncorrected, q_c (2.1–14.7) [2.5–16.5]	SCPT
Chang-Bin industrial park	0.205	2.13 (0.12)	18	Poorly graded silty sand	n/a	n/a	n/a	116.1 (11.07)	Ku et al. [56]	Taiwan	Uncorrected, q_c (1.9–8.2)[2.0–20.0]	SCPT
Nantou	0.11 (0.03)	2.38 (0.268)	8	Silty sand	n/a	n/a	n/a	119.9 (8.8)	Ku et al. [56]	Taiwan	Uncorrected, q_c (1.1–9.1)[2.0–11.0]	SCPT
Wildlife	0.15–0.25	1.93 (0.1)	5	Fine sand	n/a	n/a	n/a	100.4 (3.9)	Gillespie [32]	USA	Uncorrected, q_c (3.24–6) [3–6.36]	SCPT
Heber Road	0.10–0.12	2.435 (0.174)	10	Silty sand and fine sand	Quartz and feldspar	Angular	Holocene	123 (12.4)	Bourdeau and Amundaray [12]	USA	Uncorrected, q_c (1.77–3.1) [2.6–4.5]	SCPT
Alaska sand	0.12	n/a	n/a	Silty sandy tailings with shell fragments	n/a	Angular	Very young	135	Fear and Robertson [27]	USA	Uncorrected, q_c (n.d.) [n.d.]	SCPT

Table 3 continued

Test site	D_{50} (mm)	I_c	Nb. of data pairs	Soil description	Mineralogy	Angularity	Geologic age	$V_{s1}/Q_{tn}^{0.25}$	Author(s)	Country	q_t or q_c (MPa) (q-rang) [depth]	V_s method
Malamocco	0.072 (0.044)	2.07 (0.125)	17	Sands and silts	Calcite, dolomite, quartz and feldspar	Angular	Holocene	137.2 (15.3)	Cola and Simonini [20]	Italy	Corrected, q_t (17.9–55.4) [4.6–23.4]	SCPT
Treporti I	0.071 (0.043)	2.26 (0.35)	11	Silts	Carbonates with quartz and feldspar	Sub-angular	Holocene	140.4 (11.2)	Simonini et al. [93]	Italy	Corrected, q_t (4.2–36) [1.37–11.75]	SCPT
Treporti II	0.035 (0.015)	3.08 (0.18)	20	Silts	Carbonates with quartz and feldspar	Sub-angular	Holocene	168.7 (12.7)	Tonni and Simonini [99]	Italy	Corrected, q_t (0.7–2.6)[8.7–18.8]	SCPT
Treporti III	0.14 (0.05)	1.8	14	Fine sand	Carbonates with quartz and feldspar	Sub-angular	Holocene	123.5 (15.2)	Tonni and Simonini [99]	Italy	Corrected, q_t (4.2–10) [3–7.7]	SCPT
Rhode Island	0.033	2.708*	25	Non-plastic silt	n/a	n/a	n/a	148.3 (11.7)	Bradshaw et al. [13]	USA	Corrected, q_t (2.3–7.5) [5–33.5]	SCPT
Foynes	0.022	2.93 (0.072)	16	Marine silt	n/a	n/a	n/a	176.6 (19)	Carroll et al. [17]	Ireland	Corrected, q_t (0.45–0.68) [2.6–13.2]	SDMT

5.2 Compatibility between liquefaction charts

The applicability of the proposed V_{s1}–Q_{tn} formulations is evaluated in a different way through examining the compatibility between liquefaction charts constructed based on the proposed correlations (Eqs. 18, 19) and the various liquefaction charts found in the literature (e.g., [2, 3, 54, 62, 82]). Figures 12, 13 and 14 present some liquefaction and non-liquefaction field data from case histories involving clean sand for which V_{s1} has been calculated using the available CPT data [95] and the proposed V_{s1}–Q_{tn} formulations (Eqs. 18, 19). In particular, V_{s1} data presented in Fig. 12 ($D_{50} > 0.2$ mm) have been calculated using Eq. 19, while those presented in Figs. 13 and 14 ($D_{50} < 0.2$ mm) have been calculated using Eq. 18. In addition, Fig. 13 presents available liquefaction and non-liquefaction field case histories after Chi-Chi earthquake of 1999 [56], and Saguenay earthquake of 1988 [100] involving clean sand with V_{s1} has been calculated using the available CPT data and Eq. 18. The intervals of V_{s1}–cyclic resistance ratio (CRR) correlations of liquefaction potential based on [95] CRR–q_{c1N} relationships and transformed using Eqs. 18 and 19 are also compared to the various liquefaction charts found in the literature shown in Figs. 12, 13 and 14. For comparison, a correlation of liquefaction potential based on CRR–q_{c1N} relationships proposed by [82] and transformed using V_{s1}–q_{c1N} correlation suggested by Andrus et al. [4] is also provided in Figs. 12, 13 and 14. Figure 12 illustrates that the liquefaction interval limits based in Eq. 19 appear in much better agreement with the field data ([95] and liquefaction charts proposed by Andrus and Stokoe [2] than those proposed by Andrus and Stokoe [3], Kayen et al. [54], Lodge [62]or transformed using the correlation of [4]. Figure 13 shows that liquefaction intervals based on Eq. 18 are consistent with the field data ([56, 95, 100]) and liquefaction chart suggested by Andrus and Stokoe [3] and that transformed using the correlation of [4]. The liquefaction intervals suggested in this study, presented in Fig. 14, also appear to be in better agreement with the existing V_{s1}–CRR data points.

5.3 Evaluation of the proposed V_{s1}–Q_{tn} formulations against new field data

The applicability of the proposed V_{s1}–Q_{tn} formulations (Eqs. 18, 19) is additionally assessed by comparing the V_s profiles obtained from different field investigations at different sites with those computed by Eqs. 18 and 19. The use of the new field data, which were obtained under controlled conditions, provides independent trials of the proposed formulations. Three different sites (Burlington-

Table 4 Effect of penetration rate on cone tip resistance (Data from Krage and DeJong 2014)

Test site	Rate (mm/s)	D_{50} (mm)	q_t (Mpa)	σ_v' (kPa)	σ (kPa)	V_s (m/s)	Q_{tn}	V_{s1} (m/s)	Y
Kornbloom	20.2	0.04 – 0.07	1.13	32.5	56.1	108	18.3	143	123
	0.2		1.64				26.9		111.6
Kornbloom	20.02	0.06 – 0.07	1.875	41.7	75.1	125	27.8	155.6	120.5
	0.3		2.39				35.8		113.1
Kornbloom	20.2	0.06 – 0.07	1.50	37.1	65.6	116.5	23.48	149.3	120.6
	0.2		2.0				31.8		111.8
Lenordini	20.7	0.07	1.75	51.1	76.4	130	23.4	153.8	124.3
	0.2		2.51				34.0		113.2
Granite	20.4	0.3	5.65	139.4	155.5	176.1	46.5	162.1	110.4
	0.2		5.94				48.9		108.9

Table 5 Effect of the stress exponent, n, on V_{s1}–Q_{tn} correlations for soils with $D_{50} < 0.2$ mm

Test site	D_{50} (mm)	$Y = V_{s1}/(10 \cdot q_{t1N})^{0.25}$ q_t–corrected ($n = 0.5$)	$Y = V_{s1}/(10 \cdot Q_{tn})^{0.25}$ q_t–net ($n = 0.5$)	Difference (%)	$Y = V_{s1}/(10 \cdot Q_{tn})^{0.25}$ q_t–net ($n = 0.75$)	$Y = V_{s1}/(10 \cdot Q_{tn})^{0.25}$ q_t–net ($n = 1$)
Treporti III	0.14	122.0	123.5	1.2	121.6	116.3
	(0.05)	(15.5)	(15.2)		(15.2)	(12.9)
Heber road	0.1–0.12	122.1	123.0	0.73	115.0	108.5
		(12.7)	(12.4)		(9.1)	(7.8)
Nantou	0.11	118.7	119.9	0.80	116.8	114
	(0.03)	(9.85)	(8.80)		(9.9)	(11.6)
Malamocco	0.072	134.6	137.2	1.90	143	149.3
	(0.044)	(14.6)	(15.3)		(18.5)	(22.7)
Treporti I	0.071	138	140.4	1.70	142.4	144.8
	(0.043)	(10)	(11.2)		(13.4)	(17)
Treporti II	0.035	160.5	168.7	4.86	169.5	169.9
	(0.015)	(10.4)	(12.7)		(13.4)	(14.4)
Rhode Island	0.033	145.4	148.3	1.95	154.0	160.4
		(10.6)	(11.7)		(14.4)	(18.4)
Foynes	0.022	165.6	176.6	6.2	173.4	170.3
		(13)	(19)		(22)	(24.8)

Moran, Colchester [60], and at the eastern suburbs of New Orleans [67]) are selected for the evaluation. The advantage of these sites, in particular the first two sites (Burlington-Moran, Colchester), is that in addition to the availability of CPT data, measurements of shear wave velocity in soil and bedrock were taken using both MASW and SCPT, an issue that values the comparison and strengthens the related discussion.

The computed V_s profiles using Eqs. 18 and 19 are compared with the measured profiles at the Burlington, Colchester, and New Orleans sites in Figs. 15, 16, and 17, respectively. V_s profiles computed adopting the [4] relationship based on the available CPT data are also plotted in Figs. 15, 16, and 17 for comparison. In each

figure, the left plot corresponds to the comparison with the current study relationships, while the middle plot referred to the comparison with the [4] relationship. The right plot refers to the SBTn index profiles at each site plotted based on the available CPT data. In general, on an overall profile basis, the calculated V_s profiles based on the correlations proposed in the current study for a wide range of grain sizes ($1.0 < I_c < 4.0$) appear to work well, producing good agreement with MASW and SCPT results at the three examined sites. On the other hand, the computed profiles based on [4] relationship at Burlington–Moran (Fig. 15) and New Orleans (Fig. 17) sites match well the measured data as the soils in these two sites comprise mainly sands to silty sands with I_c of
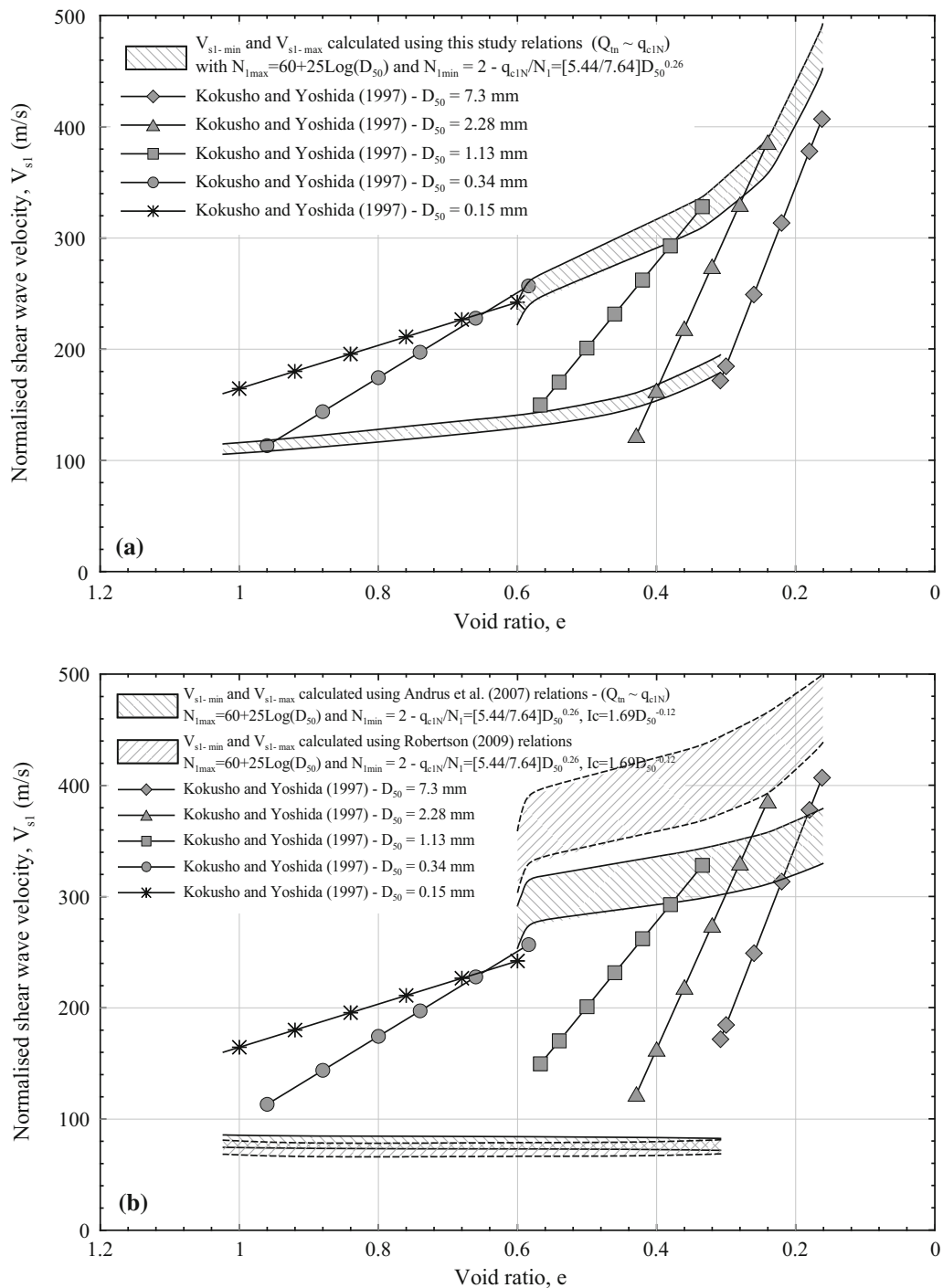
Fig. 11 Comparison of the V_{s1}–e test results [55] at different grain sizes with the V_{s1-min} and V_{s1-max} variation against e computed from: **a** the current study; **b** [4]; and [78]

1.50–2.50 (i.e., in the middle zone of Fig. 7). The data of Colchester site presented in Fig. 16 show that the [4] relationship tends to predict V_s profile somewhat lower than the V_s profiles measured by both MASW and SCPT. This underestimation of the V_s profile becomes more pronounced as the I_c increases (i.e., as the soil becomes more fine grained) in agreement with the trend of data

presented in Fig. 7. In all due fairness, the relationship by Andrus et al. [4] using wide range of soil types and grain sizes may not have been well constrained as it simply averaged the data from fine- and coarse-grained soils which appears to be not reasonable as fine- and coarse-grained soils generally follow different trends as shown in Figs. 3 and 7.

The comparative results shown in Figs. 15, 16, and 17 and the related discussion could lead us to conclude that the V_{s1}–Q_{tn} formulations suggested in the current study have a reasonable applicability to predict satisfactory the V_s profiles. In contrast, using [4] correlation or its like-minded correlations that do not impose particle-size limits for the validity of the proposed relationship would lead to inaccurate prediction of V_s profiles, especially when the test sites contain soil layers near the ends of the grain size spectrum (i.e., with extremes grain sizes).

6 Presentation using the normalized SBT chart

To explore the possibility of developing a global relationship, applicable to all uncemented, Holocene-age soils irrespective of the grain size, attempts have been made to introduce the data presented in Fig. 7 (Eqs. 21, 22) in terms of the SBTn index I_c into the normalized SBT chart proposed by Robertson [77] as shown in Fig. 18. As stated earlier, the Robertson chart makes it possible to classify the soil into nine categories ranging from sensitive, fine-grained soil to gravelly soil. The categories for normally consolidated soil generally increase with the decreasing I_c or with the increasing mean grain size (D_{50}). The data
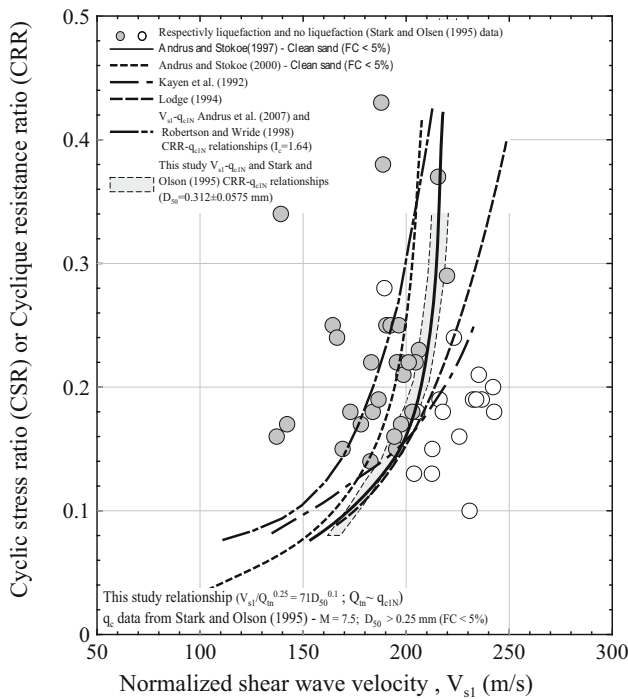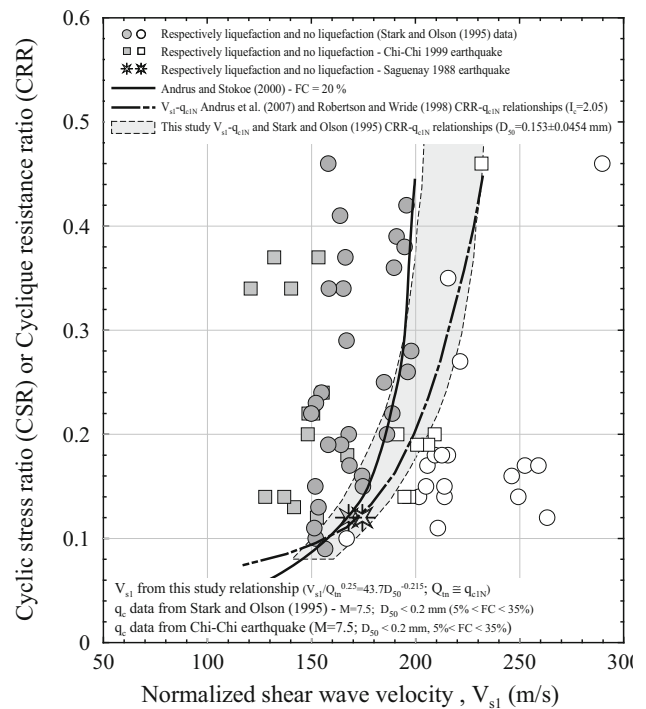

Fig. 13 Comparison of the V_{s1}–CRR data points transformed using Eq. 18 with existing correlations of liquefaction potential. CPT–CRR data from [95], Chi-Chi 1999 [56] earthquake, and Saguenay 1988 earthquake [100]. $D_{50} = 0.153$ mm
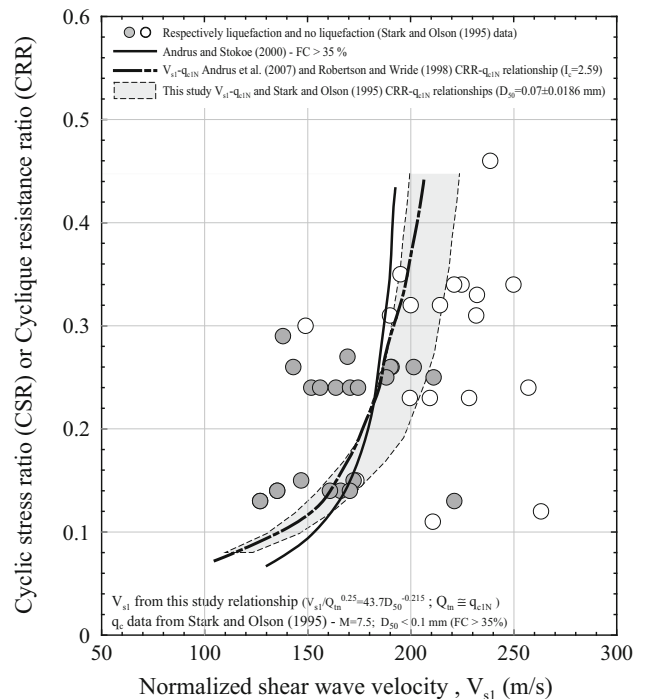

Fig. 12 Comparison of the V_{s1}–CRR data points transformed using Eq. 19 with existing correlations of liquefaction potential. CPT–CRR data from [95]. *FC* fines content; *M* earthquake magnitude. $D_{50} = 0.312$ mm

Fig. 14 Comparison of the V_{s1}–CRR data points transformed using Eq. 18 with existing correlations of liquefaction potential. CPT–CRR data from [95]. $D_{50} = 0.07$ mm
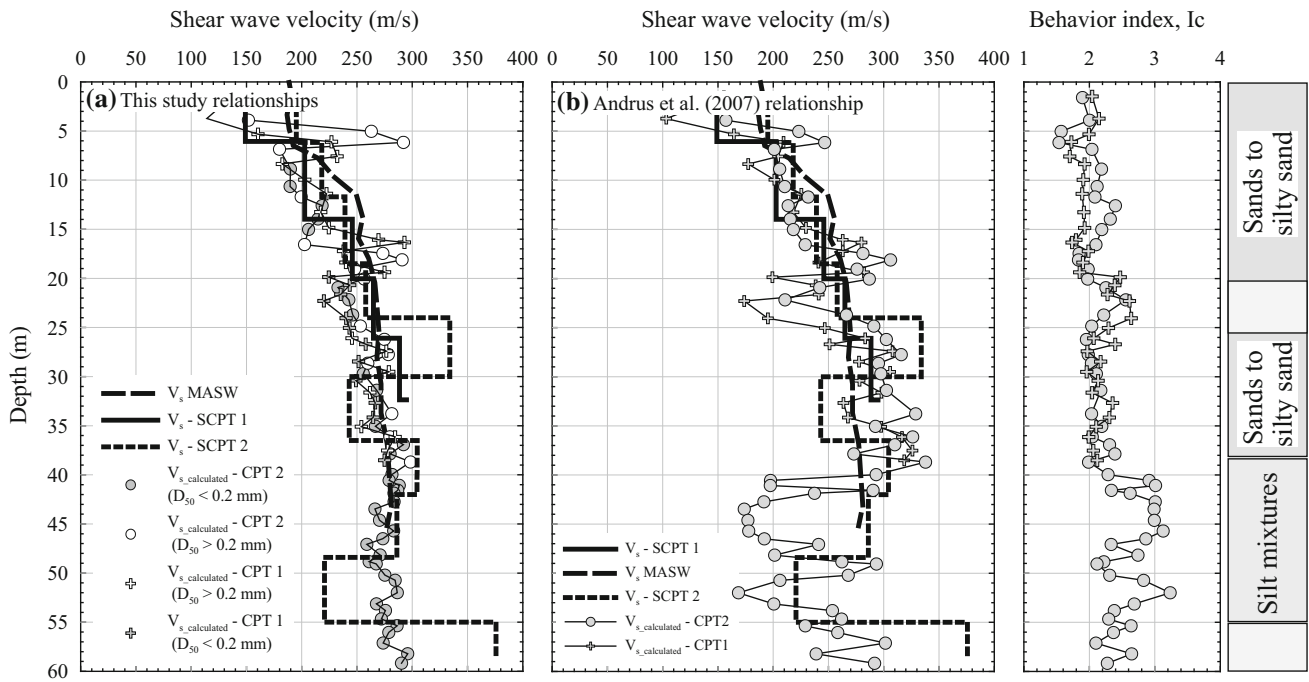
Fig. 15 Comparison between the measured V_s profiles at Burlington-Moran site with those predicted by Eqs. 18 and 19 and the relationship of [4]
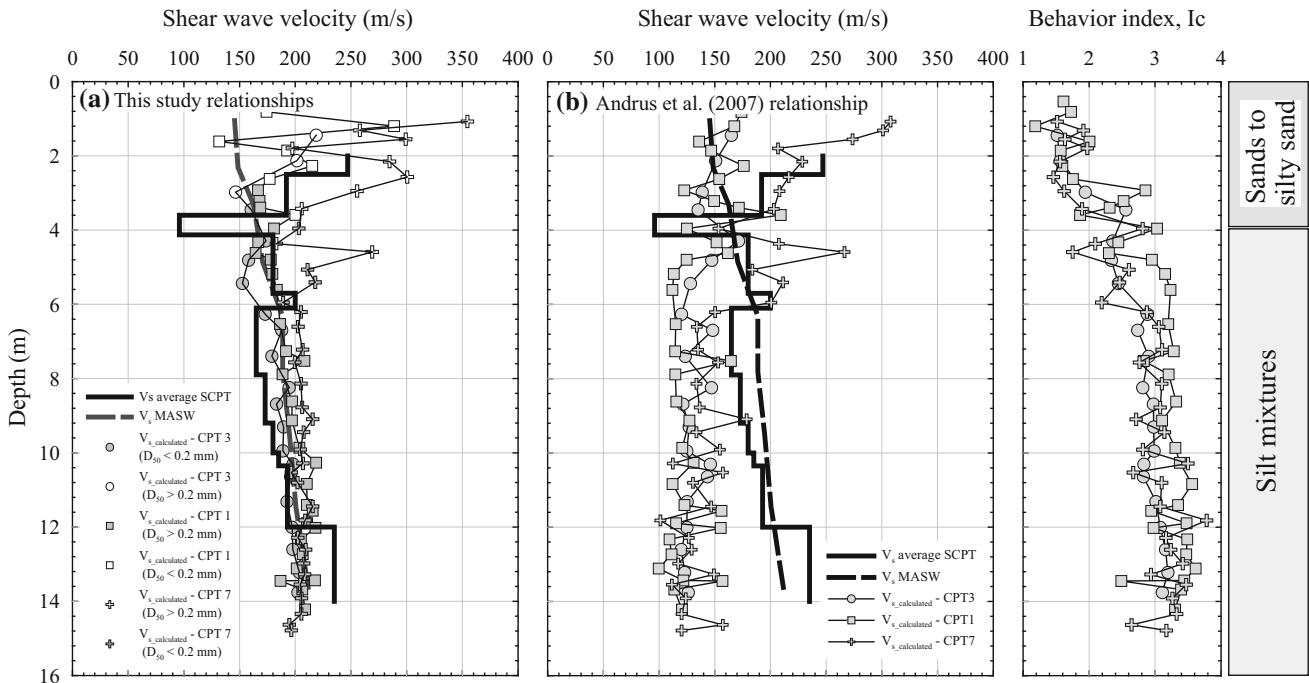

Fig. 16 Comparison between measured V_s profiles at Colchester site with those predicted by Eqs. 18 and 19 and the relationship of [4]

corresponding to the V_{s1}–Q_{tn} correlation proposed by Andrus et al. [4] and presented in Table 1 are also plotted in Fig. 18. Numbers at the ends of the solid lines (this study) and the dotted lines [4] in Fig. 18 indicate the

normalized shear wave velocity of the soil expressed in m/s. The following trends are worthy of note in Fig. 18:

1. Up to a SBT I_c value of about 2.0 and at equal normalized shear wave velocity, V_{s1}, the normalized
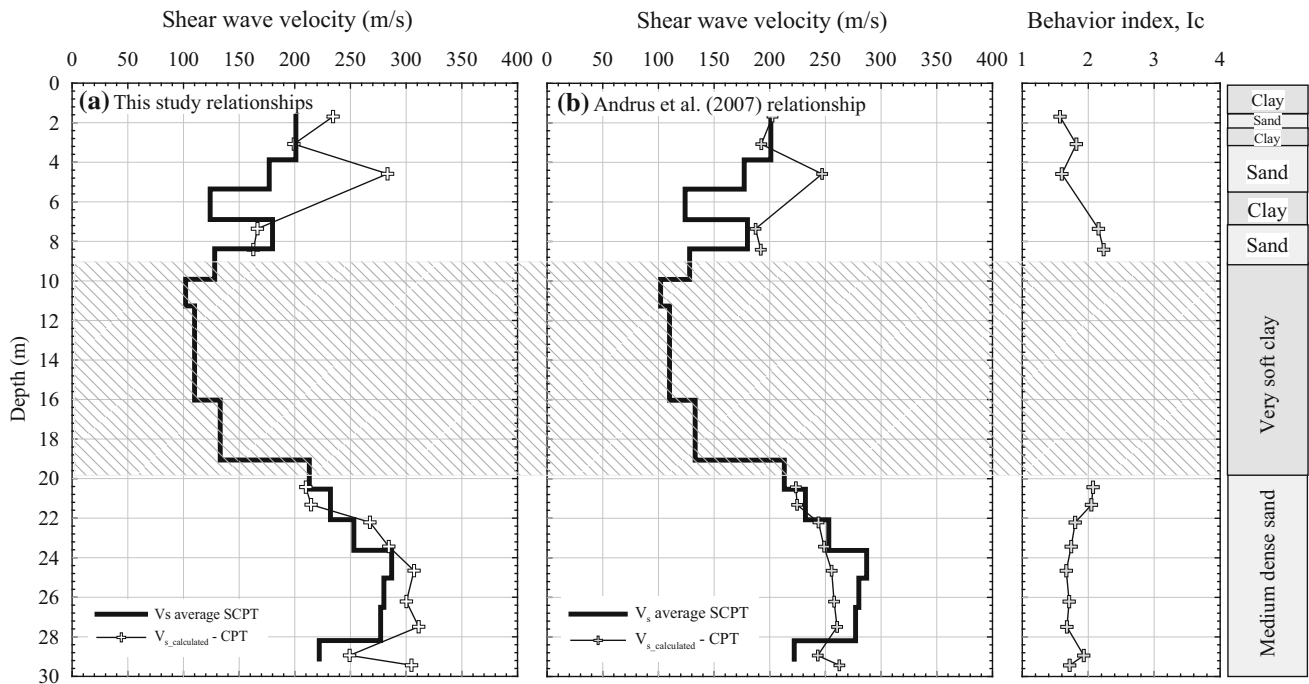
Fig. 17 Comparison between measured V_s profiles at New Orleans site with those predicted by Eqs. 18 and 19 and the relationship of [4]

penetration resistance, Q_{tn}, calculated based on the current study increases as the SBT I_c values increase (i.e., the soil becomes more fine grained).

2. This trend is totally reversed with further increase in I_c ($I_c > 2.0$). i.e., Q_{tn} decreases as the SBT I_c values increase at the same V_{s1} value.

3. The [4] relationship trends with I_c are independent of the range of I_c considered. At a given V_{s1} value, Q_{tn} calculated using [4] correlation generally decreases with the increase in I_c value. As stated earlier, [4] correlation is a unified correlation developed through an averaging of a wide range of mixed V_{s1}–Q_{tn} data including different types of soils with different particle characteristics which are different from the trend portrayed in Figs. 3 and 7. Divisions of data according to relative grain sizes would improve the accuracy of correlative equations.

4. V_{s1} values estimated based on Eqs. 21 and 22 appear to be inconsistent with the measured data. These equations generally overestimate V_{s1} of coarse-grained soils and underestimate V_{s1} of fine-grained soils. More specifically, the average measured V_{s1} values at Péribonka and Foynes sites are 275 and 153 m/s which appear to be somewhat lower and higher than those estimated based on Eqs. 21 and 22, respectively. A plausible explanation for this inconsistency is that Eqs. 21 and 22 are constructed adopting an exponential parameter of Q_{tn}-value of 0.411 which, as previously stated, does not predict properly the V_{s1} variation between the loosest and the densest state of the soil.

Therefore, estimated values of V_{s1} based on Eqs. 21 and 22 are not expected to be accurate.

7 Conclusions

Based on a wide range of well-documented case histories on different uncemented soils of Holocene age at various sites in the USA, Canada, Norway, Italy, Ireland, Taiwan, and Hong Kong, the stress-normalized shear wave velocity V_{s1} (in m/s) is defined as statistical functions of the dimensionless stress-normalized cone penetration resistance, Q_{tn}-CPT, and the mean effective diameter, D_{50}. The proposed V_{s1}–Q_{tn} correlation shows different trends with respect to particle grain sizes. For soils with $D_{50} < 0.2$ mm, the $V_{s1}/Q_{tn}^{0.25}$ ratio undergoes a significant decrease with the increase in D_{50}. This trend is completely inverted with further increase in D_{50}. These results are fully consistent with earlier results found in the literature that suggested the separation of V_s–penetration resistance correlations according to relative grain sizes.

The reversing trend of soil behavior with respect to D_{50} is not totally unknown to the geotechnical community. Some researchers reported similar soil behavior. However, the reversing trend of $V_{s1}/Q_{tn}^{0.25}$ ratio with respect to D_{50} was not previously determined because the current correlations utilize directly the main grain size, D_{50}, as a direct measurement of the soil grain size, while in constructing most of the correlations found in the literature, there are no
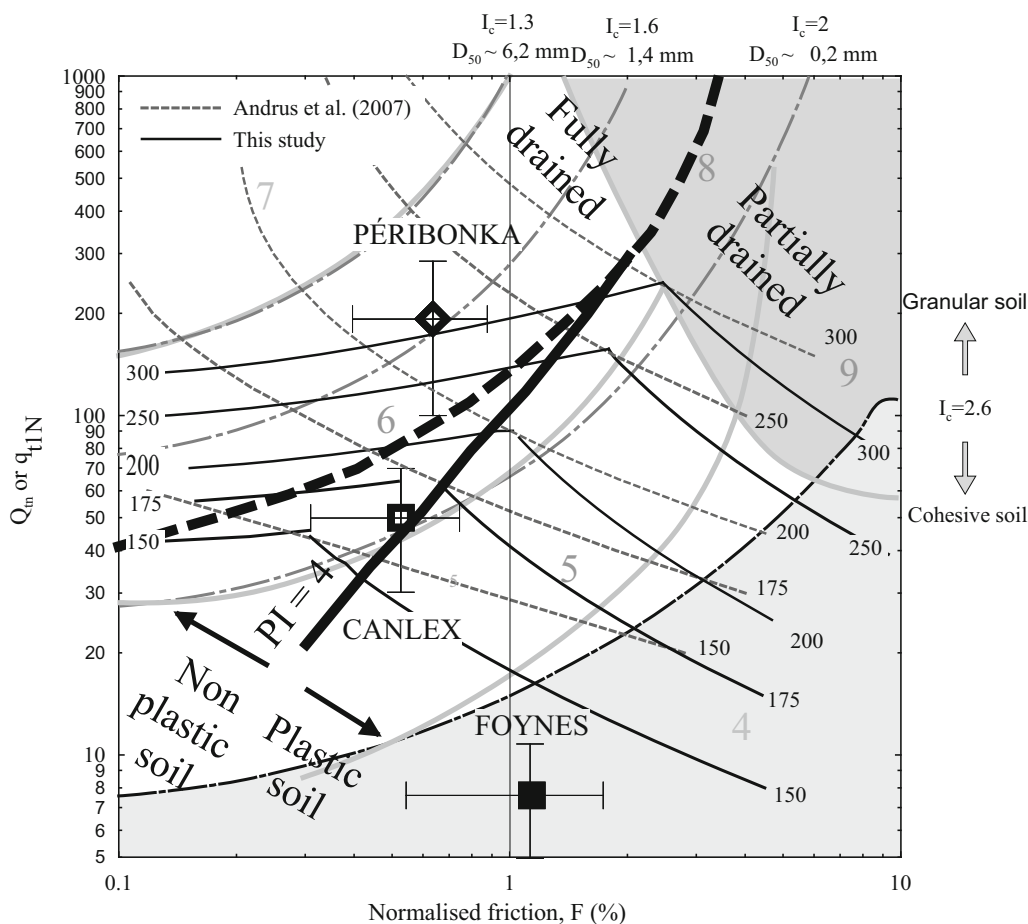
Fig. 18 Contours of normalized shear wave velocity, V_{s1} calculated based on Eqs. 21 and 22 proposed in this study and [4] on the normalized Soil Behavior Type (SBT) chart for uncemented, Holocene-age soils. The plasticity limits are reported from Cetin and Ozan (2009). The drainage condition limits are reported from [43]. The values of D_{50} are estimated from Ic using equation proposed by Karray et al. [52]

physical determination of the soil grain sizes in the field and the grain size is accessed indirectly via the Soil Behavior Type that cannot be expected to provide accurate predictions of soil grain size, but provide a guide to the mechanical characteristics (strength and stiffness) as it includes implicitly both friction ratio % F and Q_{tn}. For this particular reason, it is recommended to use the direct and the straightforward grain size measurement (i.e., D_{50}) in constructing V_s–penetration resistance correlations in the future to better account for the soil relative grain size.

The reversed trend of $V_{s1}/Q_{tn}^{0.25}$ ratio with respect to D_{50} may be attributed to several issues such as the difference in the soil compressibility (i.e., around D_{50} of 0.2 mm, soil behavior changes with respect to compressibility). It may be attributed also to the difference in the sensitivities of the parameters (V_{s1} and Q_{tn}) to grain sizes as well as the drainage conditions of the soils. In other words, the borderline between partially and fully drained soils suggested by many researchers coincides in fact with $D_{50} = 0.2$ mm.

The validity of the proposed correlations has been confirmed by comparing the calculated V_{s1} based on the proposed correlations with reliable laboratory and field measurements and examining the compatibility between the liquefaction correlations constructed based on the current formulations and the various liquefaction charts found in the literature.

References

1. Anagnostopoulous A, Koukis G, Sabatakis N, Tsiambaos G (2003) Empirical correlations of soil parameters based on cone penetration test for Greek soils. Geotech Geol Eng 21:377–387
2. Andrus RD, Stokoe KH (1997) Liquefaction resistance based on shear wave velocity. In: Youd TL, Idriss IM (eds) Proceedings of the NCEER workshop on evaluation of liquefaction resistance of soils, Salt Lake City, Utah, 5–6 January 1996. Technical Report NCEER-97- 0022. National Center for Earthquake Engineering Research, Buffalo, NY, pp 89–128
3. Andrus RD, Stokoe KH II (2000) Liquefaction resistance of soils from shear-wave velocity. J Geotech Geoenviron Eng

126(11):1015–1025. doi:10.1061/(ASCE)1090-0241(2000)126:11(1015)

4. Andrus R, Mohanan NP, Piratheepan P, Ellis BS, Holzer TL (2007) Predicting shear-wave velocity from cone penetration resistance. In: Pitilakis KD (ed) Proceedings of the 4th international conference on earthquake geotechnical engineering, Thessaloniki, Greece. Springer, The Netherlands, Paper No. 1454

5. ASTM D5778-12 (2012) Standard test method for electronic friction cone and piezocone penetration testing of soils. ASTM International, West Conshohocken, PA

6. Baldi G, Bellotti R, Ghionna V, Jamiolkwski M, Pasqualini E (1986) Interpretation of CPTs and CPTUs, 2nd part: drained penetration of sands. In: Proceedings of the 4th international geotechnical seminar, field instrumentation and in-situ measurements, Nanyang Technological Institute, Singapore, pp 143–156

7. Baldi G, Bellotti R, Ghionna VN, Jamiolkowski M, Lo Presti DCF (1989) Modulus of sands from CPTs and DMTs. In: Proceeding of the 12th international conference of soil mechanics and foundation engineering, Vol. 1, Rio de Janeiro, pp 165–170

8. Bennett MJ, You TL, Harp EL, Wieczorek GF (1981) Subsurface investigation of liquefaction, imperial valley earthquake, California, October 15, 1979, Open File Report 8 l-502. Reston, VA: US Geological Survey

9. Bernatchez L (1997) Mitochondrial DNA analysis confirms the existence of two glacial races of rainbow smelt Osmerus mordax and their reproductive isolation in the St Lawrence River estuary (Québec, Canada). Mol Ecol 6:73–83

10. Bolton MD, Gui MW, Garnier J, Corte JF, Bagge G, Laue J, Renzi R (1999) Centrifuge cone penetration tests in sand. Géotechnique 49(4):543–552

11. Bouckovalas G, Kalteziotis N, Sabatakakis N, Zervogiannis C (1989) Shear wave velocity in very soft clay. In: Proceedings of the 12th international conference on soil mechanics and foundation engineering, Rio de Janeiro (Brazil), vol. 1. Balkema, Rotterdam, pp 191–194

12. Bourdeau PL, Amundaray JI (2005) Non-parametric simulation of geotechnical variability. Géotechnique 5(2):95–108

13. Bradshaw AS, Baxter CDP, Green RA (2007) A site-specific comparison of simplified procedures for evaluating cyclic resistance of non-plastic silt, GeoDenver 2007, Geotechnical Special Publication 160, ASCE, Reston, Virginia

14. Brandenberg SJ, Bellana N, Shantz T (2010) Shear wave velocity as function of standard penetration test resistance and vertical effective stress at California bridge sites. Soil Dyn Earthq Eng 30(10):1026–1035

15. Bruzzi D, Ghionna V, Jamiolkowski M, Lancellotta R, Manfredini G (1986) Self-boring pressuremeter in Po river sand. Pressuremeter and its marine applications, STP 950, ASTM, West Conshohocken/ PA, PP 57–74

16. Bui MT (2009) Influence of some particle characteristics on the small strain response of granular materials. Ph.D. thesis, University of Southampton

17. Carroll R, Long M, Ward D (2013) Use of CPTU and SDMT to characterize silty soil. Geotechnical and Geophysical Site Characterization 4-Coutinho and Mayne (Eds), Taylor & Francis Group, London, vol 1, pp 241–249

18. Choi Y, Stewart JP (2005) Nonlinear site amplification as function of 30 m shear wave velocity. Earthq Spectra 21(1):1–30

19. Cola S, Simonini P (1999) Some remarks on the behavior of Venetian silts. In: 2nd International symposium on prefailure behaviour of geomaterials, IS Torino 99, Rotterdam: Balkema, pp 167–174

20. Cola S, Simonini P (2002) Mechanical behaviour of silty soils of the Venice lagoon as a function of their grading properties. Can Geotech J 39(4):879–893

21. Cubrinovski M, Ishihara K (1999) Empirical correlation between SPT N value and relative density for sandy soils. Soils Found 39(5):61–71

22. Cunning JC, Robertson PK, Sego DC (1995) Shear wave velocity to evaluate in situ state of cohesionless soils. Can Geotech J 32:848–858

23. Dodds JS (2003) Particle shape and stiffness-effects on soil behavior, M.Sc., thesis, Georgia Institute of Technology, Atlanta

24. Eidsmoen T, Gillespie DG, Lunne T, Campanella RG (1985) Tests with UBC seismic cone at three Norwegian research sites. UBC Department of Civil Engineering and NGI, Oslo, Norway, NGI Report No. 59040-1

25. El-Sekelly W, Abdoun T, Dobry R (2014) The use of CPT and V_s for assessment of saturated soil deposits in the centrifuge. In: Proceedings of the 8th international conference on physical modelling in geotechnics 2014 (ICPMG2014), Perth, Australia

26. Facciorusso J, Vannucchi G (2003) Application of geostatistical methods to the definition of a Liquefaction hazard map for the harbour area of Gioia Tauro. In: Proceeding of the 4th international conference on seismology and earthquake engineering, Tehran, Iran

27. Fear CE, Robertson PK (1995) Estimating the undrained strength of sand: a theoretical framework. Can Geotech J 32(5):859–870. doi:10.1139/t95-082

28. Fumal TE, Tinsley JC (1985) Mapping shear wave velocities of near surface geological materials; predicting areal limits of earthquake induced land sliding. In: Ziony TI (ed) Evaluation of earthquake hazards in the Los Angeles region—an earth science perspective, USGS Paper 1360, pp 127–150

29. Gazetas G (1991) Chapter 15: Foundation vibrations. In: Fang H-Y (ed) Foundation engineering handbook, 2nd edn. Chapman & Hall, New York, pp 553–593

30. GEI (2006) Geotechnical report-conceptual design phase national synchrotron light source II. Brookhaven National Laboratory, Upton, New York, Submitted to HDR Architecture, Inc

31. Ghionna VN, Jamiolkowski M, Pedroni S, Piccoli S (1995) Cone pressuremeter tests in Po River sand. The Pressuremeter and Its New Avenues, Balkema, pp 471–480

32. Gillespie DG (1990) Evaluation shear wave velocity and pore pressure data from the seismic cone penetration test. Ph.D. Dissertation, The University of British Columbia

33. Hanna A, Abrosii G, McConnell AD (1986) Investigation of coarse alluvial foundation for an embankment dam. Can Geotech J 23(2):203–215

34. Hardin BO (1961) Study of elastic wave propagation and damping granular materials. Ph.D. thesis, University of Florida at Gainesville, Florida

35. Hardin BO, Kalinski ME (2005) Estimating the shear modulus of gravelly soils. J Geotech Geoenviron Eng ASCE 131(7):867–875

36. Hardin BO, Richart FE (1963) Elastic wave velocities in granular soils. J Soil Mech Found Eng DivASCE 89(1):39–56

37. Harleman DRF, Bras RL, Rinaldo A, Malanotte P (2000) Blocking the Tide, Civil Engineering, ASCE, pp 52–57

38. Hegazy YA, Mayne PW (1995) Statistical correlations between Vs and cone penetration test data for different soil types. In: Proceeding of international symposium on cone penetration testing, CPT'95, Linköping (Sweden), vol. 2, pp 173–178

39. Hussien MN, Karray M (2016) Shear wave velocity as a geotechnical parameter: an overview. Can Geotech J 53(2):252–272. doi:10.1139/cgj-2014-0524

40. Ishibashi I, Sheriff MA, Cheng WL (1982) The effects of soil parameters on pore-pressure-rise and liquefaction prediction. Soils Found 22(1):39–48

41. Ishihara K (1996) Soil behaviour in earthquake geotechnics. Oxford University Press, New York. ISBN 0-19-856224-1

42. Iwasaki T, Tatsuoka F (1977) Effect of grain size and grading on dynamic shear moduli of sand. Soils Found 38(1):19–35

43. Jaeger RA, DeJong JT, Boulanger RW, Low HE, Randolph MF (2010) Variable penetration rate CPT in an intermediate soil. In: Proceeding of the 2nd international symposium cone penetration testing, Huntington Beach, CA, paper 2–50

44. Jamiolkowski M, Ladd CC, Germaine J, Lancellotta R (1985) New developments in field and lab testing of soils. In: Proceeding of the international conference on soil mechanics and foundation engineering, Vol. 1, San Francisco, pp 57–154

45. Jamiolkowski M, Ghionna VN, Lancellotta R, Pasqualini E (1988) New correlations of penetration tests for design practice. In: Proceedings of 1st international symposium on penetration testing, ISOPT-1, Orlando (USA), vol. 1. Balkema, Rotterdam, pp. 263–296

46. Jamiolkowski M, Lancellotta R, Lo Presti DCF (1995) Remarks on the stiffness at small strains of six Italian clays. In: Shibuya M, Miura (eds) Pre-failure deformation of geomaterials (vol 1, pp 817–836). Rotterdam, Balkema

47. Jefferies MG, Davies MP (1991) Soil classification by the cone penetration test: discussion. Can Geotech J 28(2):173–176

48. Jefferies MG, Davies MP (1993) Use of CPTU to estimate equivalent SPT N_{60}. Geotech Test J 16(4):458–468

49. Karray M, Éthier Y (2012) Reply to the discussion by P.K. Robertson on "Influence of particle size on the correlation between shear wave velocity and cone tip resistance". Can Geotech J 49(1):124–128. doi:10.1139/t11-101

50. Karray M, Lefebvre G (2007) Processing of the data generated by vibroflotation at the Péribonka dam, Report No. HYQG-06-03S, Report submitted to Hydro-Québec, Géowave inc., Granby, Québec, Canada

51. Karray M, Lefebvre G, Ethier Y, Bigras A (2010) Assessment of deep compaction of the Péribonka dam foundation using "modal analysis of surface waves" (MMASW). Can Geotech J 47(3):312–326. doi:10.1139/T09-108

52. Karray M, Lefebvre G, Ethier Y, Bigras A (2011) Influence of particle size on the correlation between shear wave velocity and cone tip resistance. Can Geotech J 48(4):599–615. doi:10.1139/T10-092

53. Karray M, Hussien MN, Chekired M, Ethier Y (2016) Importance of the coherence between geophysical and geotechnical data in estimating the dynamic response of soils. In: Proceedings of the 69th Canadian geotechnical conference, Vancouver, Canada, paper no. 3807

54. Kayen RE, Mitchell JK, Seed RB, Lodge A, Nishio S, Coutinho R (1992) Evaluation of SPT-CPT and shear wave-based methods for liquefaction potential assessment using Loma Prieta data. In: Proceedings of the 4th Japan–U.S. workshop on earthquake resistant design of lifeline facilities and countermeasures for soil liquefaction, Honolulu, Hawaii, 27–29 May 1992. Technical Report NCEER-92-0019. Edited by M. Hamada and T.D. O'Rourke. National Center for Earthquake Engineering Research, Buffalo, NY, pp 348–362

55. Kokusho T, Yoshida Y (1997) SPT N-value and S-wave velocity for gravelly soils with different grain size distribution. Soils Found 37(4):105–113

56. Ku C, Lee D, Wu J (2004) Evaluation of soil liquefaction in the Chi–Chi, Taiwan earthquake using CPT. Soil Dyn Earthq Eng 24:659–673

57. Ku CS, Juang CH, Ou CY (2010) Reliability of CPT I_c as an index for mechanical behavior classification of soils. Géotechnique 60(11):861–875

58. Kulhawy FH, Mayne PH (1990) Manual on estimating soil properties for foundation design. Electric Power Research Institute (EPRI), August, USA

59. Lee KM (2002) Influence of placement method on the cone penetration resistance of hydraulically placed sand-fills. Can Geotech J 39(1):592–607

60. Lens JE, Springston GE (2013) Report on the comparison of shear wave velocity measurements with Multispectral Analysis of Surface Waves (MASW) along with the Microtremor Array Method (MAM), Seismic Cone Penetration Tests (SCPT), and Standard Penetration Tests (SPT) for the Burlington and Colchester, Vermont USGS 7-1/2 Minute Quadrangles. Report Submitted to the Vermont Geological Survey

61. Lo Presti DCF, Jamiolkowski M, Pallara O, Cavallaro A, Pedroni S (1997) Shear modulus and damping of soils. Géotechnique 47(3):603–617

62. Lodge AL (1994) Shear wave velocity measurements for subsurface characterization. Ph.D. dissertation, University of California, Berkeley, Calif

63. Lunne T, Eidsmoen D, Howland JD (1986) Laboratory and field evaluation of cone penetrometer. American Society of Civil Engineers. In: Proceedings of in-situ 86, ASCE GSP 6, Blacksburg, pp 714–729

64. Lunne T, Robertson PK, Powell JJM (1997) Cone penetration testing in geotechnical practice. Blackie Academic & Professional (Chapman & Hall), Glasgow

65. MAA (2000) Soil liquefaction assessment and remediation study, phase I (Yuanlin, Dachun, and Shetou), summary report and appendixes. Taipei, Taiwan: Moh and Associates (MAA) Inc. (in Chinese)

66. Mayne PW (2006) Undisturbed sand strength from seismic cone tests. Geomechanics and Geoengineering 1(4):239–257

67. Mayne PW (2014) Interpretation of geotechnical parameters from seismic piezocone tests. Keynote Lecture. In: Robertson PK, Cabal KI (eds) Proceedings of the 3rd international symposium on cone penetration testing (CPT'14, Las Vegas), ISSMGE Technical Committee TC 102, pp 47–73

68. Mayne PW, Rix GJ (1993) G_{max}–q_c relationships for clays. Geotech Test J 16(1):54–60

69. Mayne PW, Rix GJ (1995) Correlations between shear wave velocity and cone tip resistance in natural clays. Soils Found 35(2):107–110

70. Mayne PW, Mitchell JK, Auxt JA, Yilmaz R (1995) U.S. national report on CPT. In: Proceedings of symposium on cone penetration testing, Vol. 1, Swedish Geotechnical Society, pp 263–276

71. Menq FY (2003) Dynamic properties of sandy and gravelly soils. Ph.D. Dissertation, The University of Texas at Austin

72. Mitchell J, Soga K (2005) Fundamentals of soil behavior, 3rd edn. Wiley, New York

73. Mullen WG (1991) An evaluation of the utility of four in-situ test methods for transmission line foundation design, Ph.D. dissertation, School of Civil Engineering, Virginia Polytechnic Institute, Blacksburg

74. Ohta Y, Goto N (1978) Empirical shear wave velocity equations in terms of characteristic soil indices. Earthq Eng Struct Dyn 6:167–187

75. Piratheepan P (2002) Estimating shear-wave velocity from SPT and CPT data. MSc. thesis, Clemson University

76. Rix GJ, Stokoe KH (1991) Correlation of initial tangent moduli and cone penetration resistance. In: Huang AB (ed) Calibration chamber testing. Elsevier, New York, pp 351–362

77. Robertson PK (1990) Soil classification using the cone penetration test. Can Geotech J 27(1):151–158

78. Robertson PK (2009) Interpretation of cone penetration tests—a unified approach. Can Geotech J 46:1337–1355

79. Robertson PK (2012) Discussion of "Influence of particle size on the correlation between shear wave velocity and cone tip resistance". Can Geotech J 48(4):599–615

80. Robertson PK, Cabal KL (2010) Guide to cone penetration testing for geotechnical engineering, 3rd edn, Gregg Drilling and Testing, Signal Hill, California

81. Robertson PK, Campanella RG (1983) Interpretation of cone penetration tests—part I (sand). Can Geotech J 20(4):718–733

82. Robertson PK, Wride CE (1998) Evaluating cyclic liquefaction potential using the cone penetration test. Can Geotech J 35(3):442–459

83. Robertson PK, Campanella RG, Gillespie D, Greig J (1986) Use of piezometer cone data. In-Situ'86 use of in-s-itu testing in geotechnical engineering, GSP 6, ASCE, Reston, VA, Specialty Publication, SM 92, pp 1263–1280

84. Robertson PK, Woeller DJ, Kokan M, Hunter J, Luternaur J (1992) Seismic techniques to evaluate liquefaction potential. In: Proceedings of the 45th Canadian geotechnical conference, Toronto, Ont., pp 5-1–5-9

85. Robertson PK, Wride CE, List BR, Atukorala U, Biggar KW, Byrne PM, Campanella RG, Cathro DC, Chan DH, Czajewski K, Finn WDL, Gu WH, Hammamji Y, Hofmann BA, Howie JA, Hughes J, Imrie AS, Konrad JM, Küpper A, Law T, Lord ERF, Monahan PA, Morgenstern NR, Phillips R, Piché R, Plewes HD, Scott D, Sego DC, Sobkowicz J, Stewart PA, Watts BD, Woeller DJ, Youd TL, Zavodni Z (2000) The CANLEX project: summary and conclusions. Can Geotech J 37:563–591

86. Roesler SK (1979) Anisotropic shear modulus due to stress anisotropy. J Geotech Eng Div ASCE 105(7):871–880

87. Rollins KM, Evans MD, Diehl NB, Daily WD (1998) Shear modulus and damping relationships for gravels. J Geotech Geoenviron Eng 124(5):396–405

88. Santamarina JC, Aloufi M (1999) Micro-scale interpretation of wave propagation in soils–fabric and fabric changes. In: Proceedings of the 2nd international symposium on pre-failure deformation characteristics of geomaterials—ISTORINO99, vol. 2. Balkema, Rotterdam, pp 451–458

89. Santamarina JC, Klein KA, Fam MA (2001) Soils and waves. Wiley, Chichester

90. Schneider JA, McGillivray AV, Mayne PW (2004) Evaluation of SCPTU intra-correlations at sand sites in the Lower Mississippi River valley, USA, Geotechnical & Geophysical Site Characterization, Vol. 1, (Proc. ISC-2, Porto), Millpress, Rotterdam, pp 1003–1010

91. Shen CK, Lee KM, Li XS (1997) Hydraulic fill performance in Hong Kong-Phase 2. GEO Report 64, Geotechnical Engineering Office, Civil Engineering Department, Government of the Hong Kong Special Administrative Region, Hong Kong. Can be ordered at www.info.gov.hk/ced/eng/publications/

92. Simonini P (2004) Characterization of the Venice lagoon silts from in-situ tests and the performance of a test embankment. Keynote Lecture. In: Proceedings of ISC'02, geotechnical and geophysical site characterization. Porto, 1. Rotterdam: Millpress, pp 187–207

93. Simonini P, Ricceri G, Cola S (2007) Geotechnical characterization and properties of Venice lagoon heterogeneous silts. In: Tan TS, Phoon KK, Hight DW, Leroueil S (eds) Characterization and engineering properties of natural soils, pp 2289–2328

94. Skempton AW (1986) Standard penetration test procedures and the effects in sands of overburden pressure, relative density, particle size, aging and overconsolidation. Géotechnique 36(3):425–557

95. Stark TD, Olson SM (1995) Liquefaction resistance using CPT and field case histories. ASCE J Geotech Eng 121(12):856–869

96. Suzuki Y, Sanematsu T, Tokimatsu K (1998) Correlation between SPT and seismic CPT. In: Proceedings of the first international conference on geotechnical site characterization, Atlanta, Ga., 19–22 April 1998. Balkema, Rotterdam, the Netherlands. pp 1375–380

97. Sykora DW (1987) Examination of existing shear wave velocity and shear modulus correlations in soils, Department of the Army, Waterways Experiment Station, Corps of Engineers, Miscellaneous Paper GL-87-22

98. Sykora DE, Stokoe KH (1983) Correlations of in-situ measurements in sands of shear wave velocity. Soil Dyn Earthq Eng 20:125–136

99. Tonni L, Simonini P (2013) Shear wave velocity as function of cone penetration test measurements in sand and silt mixtures. Eng Geol 163:55–67

100. Tuttle M, Law KT, Seeber L, Jacob K (1990) Liquefaction and ground failure induced by the 1988 Saguenay, Quebec, Earthquake. Can Geotech J 27(5):580–589

101. Wichtmann T, Triantafyllidis TH (2009) Influence of the grain size distribution curve of quartz sand on the small strain shear modulus G_{max}. J Geotech Geoenviron Eng ASCE 135(10):1404–1418

102. Wride CE, Robertson PK, Biggar RG, Campanella RG, Hofmann BA, Hughes JMO, Kupper A, Woeller DJ (2000) Interpretation of in situ test results from the CANLEX sites. Can Geotech J 37(3):505–529

103. Youd TL et al (2001) Liquefaction resistance of soils: summary report from the 1996 NCEER and 1998 NCEER/NSF workshops on evaluation of liquefaction resistance of soils. J Geotech Geoenviron Eng 127(10):817–833

104. Zhang G, Robertson PK, Brachman RWI (2002) Estimating liquefaction-induced ground settlements from CPT for level ground. Can Geotech J 39(5):1168–1180